treatment for patients with advanced HCC [31]. To improve the treatment efficacy, further chemotherapy regimens, such as the combination therapy comprising TAI with cisplatin suspended in lipiodol and sorafenib or other molecularly targeted agents, remain as challenges to be met following further detailed investigations. These findings may be helpful in predicting the life expectancy in HCC patients treated with TAI and provide more information to stratify patients in future TAI trials. It is also important to validate this prognostic index by applying it to other populations of HCC patients.

In conclusion, TAI with cisplatin suspended in lipiodol exhibited favorable tumor efficacy and survival in patients with HCC. Although no specific prognostic factors for TAI could be identified in this study, the results of the prognostic factors and the prognostic index may be helpful for predicting life expectancy, determining the most appropriate treatment strategies, and designing future clinical trials.

## References


1. Llovet JM, Burroughs A, Bruix J. Hepatocellular carcinoma. Lancet. 2003;362:1907–17.
2. Cammà C, Schepis F, Orlando A, Albanese M, Shahied L, Trevisani F, et al. Transarterial chemoembolization for unresectable hepatocellular carcinoma: meta-analysis of randomized controlled trials. Radiology. 2002;224:47–54.
3. Llovet JM, Bruix J. Systematic review of randomized trials for unresectable hepatocellular carcinoma: chemoembolization improves survival. Hepatology. 2003;37:429–42.
4. Lin DY, Liaw YF, Lee TY, Lai CM. Hepatic arterial embolization in patients with unresectable hepatocellular carcinoma—a randomized controlled trial. Gastroenterology. 1988;94:453–6.
5. Pelletier G, Roche A, Ink O, Anciaux ML, Derhy S, Rougier P, et al. A randomized trial of hepatic arterial chemoembolization in patients with unresectable hepatocellular carcinoma. J Hepatol. 1990;11:181–4.
6. Groupe d'Etude et de Traitement du Carcinome Hepatocellulaire. A comparison of lipiodol chemoembolization and conservative treatment for unresectable hepatocellular carcinoma. N Engl J Med. 1995;332:1256–61.
7. Pelletier G, Ducreux M, Gay F, Luboinski M, Hagege H, Dao T, et al. Treatment of unresectable hepatocellular carcinoma with lipiodol chemoembolization: a multicenter randomized trial. J Hepatol. 1998;29:129–34.
8. Bruix J, Llovet JM, Castells A, Montana X, Bru C, Ayuso MC, et al. Transarterial embolization versus symptomatic treatment in patients with advanced hepatocellular carcinoma: results of a randomized controlled trial in a single institution. Hepatology. 1998;27:1578–83.
9. Lo CM, Ngan H, Tso WK, Liu CL, Lam CM, Poon RT, et al. Randomized controlled trial of transarterial lipiodol chemoembolization for unresectable hepatocellular carcinoma. Hepatology. 2002;35:1164–71.
10. Llovet JM, Real MI, Montana X, Planas R, Coll S, Aponte J, et al. Arterial embolisation or chemoembolisation versus symptomatic treatment in patients with unresectable hepatocellular carcinoma: a randomised controlled trial. Lancet. 2002;359:1734–9.
11. Schwartz JD, Beutler AS. Therapy for unresectable hepatocellular carcinoma: review of the randomized clinical trials-II: systemic and local non-embolization-based therapies in unresectable and advanced hepatocellular carcinoma. Anticancer Drugs. 2004;15:439–52.
12. Minagawa M, Makuuchi M. Treatment of hepatocellular carcinoma accompanied by portal vein tumor thrombus. World J Gastroenterol. 2006;12:7561–7.
13. Imaeda T, Yamawaki Y, Seki M, Goto H, Iinuma G, Kanematsu M, et al. Lipiodol retention and massive necrosis after lipiodol-chemoembolization of hepatocellular carcinoma: correlation between computed tomography and histopathology. Cardiovasc Intervent Radiol. 1993;16:209–13.
14. Takayasu K, Shima Y, Muramatsu Y, Moriyama N, Yamada T, Makuuchi M, et al. Hepatocellular carcinoma: treatment with intraarterial iodized oil with and without chemotherapeutic agents. Radiology. 1987;163:345–51.
15. Okusaka T, Okada S, Ueno H, Ikeda M, Yoshimori M, Shimada K, et al. Evaluation of the therapeutic effect of transcatheter arterial embolization for hepatocellular carcinoma. Oncology. 2000;58:293–9.
16. Okusaka T, Sato T, Hinotsu S, Shioyama Y, Kasugai H, Tanaka K, et al. Transarterial infusion chemotherapy alone versus transarterial chemoembolization for the treatment of hepatocellular carcinoma: results of a multicenter randomized phase III trial. J Clin Oncol 2007 ASCO Annual Meeting Proceedings. 2007;25:18S (abstr 4643).
17. Ikeda M, Maeda S, Shibata J, Muta R, Ashihara H, Tanaka M, et al. Transcatheter arterial chemotherapy with and without embolization in patients with hepatocellular carcinoma. Oncology. 2004;66:24–31.
18. Okusaka T, Okada S, Ueno H, Ikeda M, Iwata R, Furukawa H, et al. Transcatheter arterial embolization with zinostatin stimalamer for hepatocellular carcinoma. Oncology. 2002;62:228–33.
19. Yamasaki T, Kimura T, Kurokawa F, Aoyama K, Ishikawa T, Tajima K, et al. Prognostic factors in patients with advanced hepatocellular carcinoma receiving hepatic arterial infusion chemotherapy. J Gastroenterol. 2005;40:70–8.
20. Uka K, Aikata H, Takaki S, Miki D, Kawaoka T, Jeong SC, et al. Pretreatment predictor of response, time to progression, and survival to intraarterial 5-fluorouracil/interferon combination therapy in patients with advanced hepatocellular carcinoma. J Gastroenterol. 2007;42:845–53.
21. Yoshikawa M, Ono N, Yodono H, Ichida T, Nakamura H. Phase II study of hepatic arterial infusion of a fine-powder formulation of cisplatin for advanced hepatocellular carcinoma. Hepatol Res. 2008;38:474–83.
22. Lladó L, Virgili J, Figueras J, Valls C, Dominguez J, Rafecas A, et al. A prognostic index of the survival of patients with unresectable hepatocellular carcinoma after transcatheter arterial chemoembolization. Cancer. 2000;88:50–7.
23. Ikeda M, Okada S, Yamamoto S, Sato T, Ueno H, Okusaka T, et al. Prognostic factors in patients with hepatocellular carcinoma treated by transcatheter arterial embolization. Jpn J Clin Oncol. 2002;32:455–60.
24. Changchien CS, Chen CL, Yen YH, Wang JH, Hu TH, Lee CM, et al. Analysis of 6381 hepatocellular carcinoma patients in southern Taiwan: prognostic features, treatment outcome, and survival. J Gastroenterol. 2008;43:159–70.
25. Shibata J, Fujiyama S, Sato T, Kishimoto S, Fukushima S, Nakano M. Hepatic arterial injection chemotherapy with cisplatin suspended in an oily lymphographic agent for hepatocellular carcinoma. Cancer. 1989;64:1586–94.
26. Yoshikawa M, Saisho H, Ebara M, Iijima T, Iwama S, Endo F, et al. A randomized trial of intrahepatic arterial infusion of 4′-epidoxorubicin with lipiodol versus 4′-epidoxorubicin alone in

the treatment of hepatocellular carcinoma. Cancer Chemother Pharmacol. 1994;33(Suppl):S149–52.
27. Okusaka T, Okada S, Nakanishi T, Fujiyama S, Kubo Y. Phase II trial of intra-arterial chemotherapy using a novel lipophilic platinum derivative (SM-11355) in patients with hepatocellular carcinoma. Invest New Drugs. 2004;22:169–76.
28. Okuda K, Ohtsuki T, Obata H, Tomimatsu M, Okazaki N, Hasegawa H, et al. Natural history of hepatocellular carcinoma and prognosis in relation to treatment. Study of 850 patients. Cancer. 1985;56:918–28.
29. Pugh RNH, Murry-Lyon IM, Dawson JL, Pietroni MC, Williams R. Transection of the oesophagus for bleeding oesophageal varices. Br J Surg. 1973;60:646–9.
30. Luo KZ, Itamoto T, Amano H, Oshita A, Ushitora Y, Tanimoto Y, et al. Comparative study of the Japan Integrated Stage (JIS) and modified JIS score as a predictor of survival after hepatectomy for hepatocellular carcinoma. J Gastroenterol. 2008;43:369–77.
31. Llovet JM, Ricci S, Mazzaferro V, Hilgard P, Gane E, Blanc JF, et al. SHARP Investigators Study Group. Sorafenib in advanced hepatocellular carcinoma. N Engl J Med. 2008;359:378–90.

STEM CELLS®

EMBRYONIC STEM CELLS/INDUCED PLURIPOTENT STEM CELLS

# Characterization of Dendritic Cells and Macrophages Generated by Directed Differentiation from Mouse Induced Pluripotent Stem Cells

SATORU SENJU,[a,b] MIWA HARUTA,[a,b] YUSUKE MATSUNAGA,[a,b] SATOSHI FUKUSHIMA,[a,b] TOKUNORI IKEDA,[a,b] KAZUTOSHI TAKAHASHI,[c] KEISUKE OKITA,[c] SHINYA YAMANAKA,[c,d] YASUHARU NISHIMURA[a]

[a]Department of Immunogenetics, Kumamoto University Graduate School of Medical Sciences, Kumamoto, Japan; [b]Japan Science and Technology Agency, CREST, Tokyo, Japan; [c]Center for iPS Cell Research and Application, Institute for Integrated Cell-Material Sciences, and [d]Department of Stem Cell Biology, Institute for Frontier Medical Sciences, Kyoto University, Kyoto, Japan

**Key Words.** Induced pluripotent stem cells • Dendritic cells • Macrophages • MHC • Embryonic stem cells • Cell therapy

ABSTRACT

**Methods have been established to generate dendritic cells (DCs) from mouse and human embryonic stem (ES) cells. We designated them as ES-DCs and mouse models have demonstrated the induction of anti-cancer immunity and prevention of autoimmune disease by in vivo administration of genetically engineered ES-DCs. For the future clinical application of ES-DCs, the histoincompatibility between patients to be treated and available human ES cells and the ethical concerns associated with human ES cells may be serious obstacles. However, recently developed induced pluripotent stem (iPS) cell technology is expected to resolve these issues. This report describes the generation and characterization of DCs derived from mouse iPS cells. The iPS cell-derived DCs (iPS-DCs) possessed the characteristics of DCs including the capacity of T-cell-stimulation, antigen-processing and presentation and cytokine production. DNA microarray analyses revealed the upregulation of genes related to antigen-presenting functions during differentiation into iPS-DCs and similarity in gene expression profile in iPS-DCs and bone marrow cell-derived DCs. Genetically modified iPS-DCs expressing antigenic protein primed T-cells specific to the antigen in vivo and elicited efficient antigen-specific antitumor immunity. In addition, macrophages were generated from iPS cells (iPS-MP). iPS-MP were comparable with bone marrow cell-derived macrophages in the cell surface phenotype, functions, and gene expression profiles.** STEM CELLS *2009;27:1021–1031*

Disclosure of potential conflicts of interest is found at the end of this article.

## INTRODUCTION

Dendritic cells (DCs) are the most potent antigen-presenting cells (APC) which are known to play major roles in the priming of naive T-cells and also in the maintenance of immunological self-tolerance, by promoting T-cells with regulatory functions or by inducing anergy of T-cells. Several groups have previously established methods to generate APC or DCs from mouse [1, 2] and human [3–5] embryonic stem (ES) cells (ES-DCs). Genetic engineering of ES-DCs can readily be done by the introduction of transgenes into undifferentiated ES cells and subsequent differentiation of the ES cell clones into ES-DCs. By genetic engineering, we can generate ES-DCs capable of modulating immune response in an antigen-specific manner. Mouse systems have demonstrated the induction of anti-cancer immunity [6–10] and the prevention of autoimmune disease [11, 12] by in vivo administration of genetically engineered ES-DCs.

Considering the future clinical application of ES-DCs technology, however, the unavailability of human ES cells genetically identical to the patients to be treated is a problem. In addition, ethical concerns related to the use of human ES cells are anticipated to be serious obstacles which will hinder the realization of the medical use of human ES-DCs.

It was recently revealed that ES cell-like pluripotent stem cells, designated as induced pluripotent stem (iPS) cells, can be generated by the simultaneous introduction of several genes for reprogramming factors, such as Oct3/4, Sox2, Klf4, and c-Myc, into somatic cells [13–20]. The issue of histoincompatibility between patients to be treated and ES cells may be overcome by the generation of iPS cells from somatic cells of the patients such as fibroblasts. The major ethical issues related to human ES cells would be avoided by aid of iPS cell technology, because the use of human embryos is not necessary for the generation of iPS cells.

Author contributions: S.S.: conception and design, collection of data, manuscript writing, final approval of manuscript; M.H., Y.M., S.F., and T.I.: collection of data, final approval of manuscript; K.T., K.O., and S.Y.: provision of study material, final approval of manuscript; Y.N.: manuscript writing, final approval of manuscript.

Correspondence: Satoru Senju, M.D., Ph.D., Department of Immunogenetics, Graduate School of Medical Sciences, Kumamoto University, Honjo 1-1-1, Kumamoto 860-8556, Japan. Telephone: +81-96-373-5313; Fax: +81-96-373-5314; e-mail: senjusat@gpo.kumamoto-u.ac.jp Received October 9, 2008; accepted for publication February 12, 2009; first published online in STEM CELLS *EXPRESS* February 13, 2009; available online without subscription through the open access option.  1066-5099/2009/$30.00/0 doi: 10.1002/stem.33

Differentiation of iPS cells into various cells belonging to the three germ layers has been demonstrated by the analysis of teratomas generated from mouse and human iPS cells. In addition, the pluripotency of iPS cells is obvious by the contribution of iPS cell-derived cells to various organs of the chimeric mice developed from iPS cell-introduced blastocysts [14]. As for the in vitro generation of cells of mesodermal lineage from iPS cells, differentiation into cardiac myocytes and endothelial cells from mouse iPS cells has been recently reported [21–23]. However, it remains to be elucidated whether fully differentiated and functional hematopoietic cells can be generated from iPS cells by directed differentiation in vitro. In the present study, we generated DCs and macrophages from mouse iPS cells (iPS-DCs and iPS-MP), and characterized them by morphological, functional, and gene-expression analyses.

## Materials and Methods

### Cell Lines, Cytokines, Chemicals, and Peptides

The mouse embryonic fibroblast-derived iPS cell lines were maintained in Dulbecco's modified Eagle's medium (DMEM) containing 15% ES cell-qualified fetal calf serum (FCS; Gibco-Invitrogen, Carlsbad, CA; http://www.invitrogen.com), 1,000 U/ml leukemia inhibitory factor, 50 U/ml penicillin, 50 mg/ml streptomycin, nonessential amino acids, and 50 $\mu$M 2-mercaptoethanol (2-ME) on feeder cell layers of mitomycin C-treated mouse primary embryonic fibroblasts (PEF). Mouse bone marrow stromal cells, OP9 [24], were maintained in DMEM supplemented with 20% FCS and seeded onto gelatin-coated dishes before used as feeder cells. The T-cell hybridomas, RF33.70 [25], recognizing ovalbumin $(OVA)_{257-264}$ in the context of $K^b$ and DO11.10[26], recognizing $OVA_{323-339}$ in the context of I-$A^d$, were maintained in RPMI-1640 medium supplemented with 10% FCS. MO4 [27], a C57BL/6-derived B16 melanoma cell line expressing OVA, was maintained in RPMI-1640 medium supplemented with 10% horse serum. Recombinant mouse interleukin (IL)-4, tumor necrosis factor (TNF)-$\alpha$, granulocyte macrophage colony stimulating factor (GM-CSF) and macrophage colony stimulating factor (M-CSF) were purchased from Peprotec (London, U.K.; http://www.peprotechec.com). Lipopolysaccharide (LPS) from *Escherichia coli* and OVA protein was purchased from Sigma Chemical (St. Louis, MO; http://www.sigma-chem.com.au), agonistic anti-CD40 monoclonal antibody (mAb, clone HM-40-3) was from PharMingen (San Jose, CA; http://www.bdbiosciences.com) and OK432 was purchased from Chugai Pharmaceutical (Tokyo, Japan; http://www.chugai-pharm.co.jp/hc/chugai_top_en.jsp). $OVA_{257-264}$ peptide, SIINFEKL, was synthesized on an automatic peptide synthesizer (PSSM8; Shimadzu, Kyoto, Japan; http://www.shimadzu.com) and purified by HPLC.

### Differentiation Culture

The procedure for induction of differentiation of iPS cells into DCs is composed of three steps (supporting information Fig. 1). Step 1: iPS cells were suspended in $\alpha$-MEM supplemented with 20% FCS and seeded ($1 \times 10^5$ cells per dish) onto OP9 cell layers in 100-mm dishes. On day 6 or 7, the cells were treated with PBS/0.25% trypsin/1 mM ethylenediaminetetraacetic acid (EDTA; trypsin/EDTA) for 10 minutes, recovered with medium containing FCS, and subjected to step 2 culture or stocked frozen for future use. Step 2: Cells harvested from step 1 culture were suspended in $\alpha$-MEM supplemented with 20% FCS, GM-CSF (1,000 U/ml), and 2-ME (50 $\mu$M) and plated onto freshly prepared OP9 cell layers. Cells recovered from one dish of step 1 culture were seeded onto 8–10 dishes. Thereafter, at 6 days after the passage, floating cells were recovered by pipetting and then were subjected to step 3 culture or stocked frozen. Step 3: The cells were transferred to bacteriological Petri dishes ($5 \times 10^5$ cells/100-mm dish) without feeder cells and cultured in RPMI-1640 medium supplemented with 10% FCS, GM-CSF (1,000 U/ml) and 2-ME. To induce complete maturation of iPS-DCs, cells cultured for 10–14 days in Petri dishes were transferred to new dishes and cultured in RPMI-1640/10% FCS supplemented with GM-CSF (1,000 U/ml), IL-4 (10 ng/ml), TNF-$\alpha$ (5 ng/ml), and anti-CD40 mAb (10 $\mu$g/ml). For the generation of macrophages, the cells recovered from step 2 were cultured in bacteriological Petri dishes or tissue culture-coated dishes ($1–2 \times 10^6$ cells/100-mm dish) in RPMI-1640 medium supplemented with 10% FCS, 5% horse serum, M-CSF (100 ng/ml), and 2-ME.

### Generation of DCs and Macrophages From Bone Marrow Cells

Femoral and tibial bone marrow cells were obtained from DBA/2 mice. To generate DCs (BM-DCs), cells were cultured in RPMI-1640 medium supplemented with 10% FCS, 1,000 U/ml GM-CSF, and 50 $\mu$M 2-ME for 7 days in Petri dishes. To generate macrophages (BM-MP), cells were cultured in RPMI-1640 medium supplemented with 10% FCS, 5% horse serum, 100 ng/ml M-CSF, and 50 $\mu$M 2-ME for 7–10 days in Petri dishes. For the analysis, macrophages were harvested using trypsin/EDTA.

### Microscopic Analysis

Unfixed cells in the culture plates were stained with phycoerythrin (PE)-conjugated anti-Flk1 monoclonal antibody (1.25 $\mu$g/ml) in DMEM supplemented with 10% FCS for 1 hour and washed three times. Cytospin specimens were stained with May-Grünwald-Giemsa and mounted in Entellan *neu* (Merck, Darmstadt, Germany; http://www.merck.com). Bright-field, phase-contrast, and fluorescence microscopic analysis were done on an inverted microscope (IX70, Olympus, Tokyo, Japan, http://www.olympus-global.com/en/global) and microscopic images were captured by using a digital camera unit DP70 (Olympus).

### Flow Cytometric Analysis

The staining of cells and analysis on a flow cytometer (FACScan, Becton Dickinson, San Jose, CA; http://www.bd.com) was done as described previously [2]. The following monoclonal antibodies (mAb) conjugated with fluorescence isothiocyanate (FITC) or PE were used for staining: anti-mouse Flk-1 (clone Avas12a1, rat IgG2a, eBioscience, San Diego, CA; http://www.ebioscience.com), anti-mouse CD45 (clone 30-F11, rat IgG2b, eBioscience), anti-mouse CD11b (clone M1/70, IgG2b, Pharmingen), anti-mouse CD11c (clone N148, hamster IgG, Chemicon, Temecula, CA, http://www.chemicon.com), anti-mouse CD80 (clone RMMP-1, rat IgG2a, Caltag), anti-mouse CD86 (clone RMMP-2, rat IgG2a, Caltag), anti-F4/80 (A3-1, rat IgG2b, Serotec Ltd., Oxford, U.K., http://www.serotec.com), mouse IgG2a control (clone G155-178, Pharmingen), mouse IgG2a control (clone G155-178, Pharmingen), rat IgG2a control (clone LO-DNP-16, Caltag), rat IgG2a control (clone LODNP-57, Beckman-Coulter, Fullerton, CA, http://www.beckmancoulter.com), and hamster IgG control (clone 530-6, Caltag). Intracellular staining with FITC-conjugated Fab fragment of anti-influenza virus hemagglutinin (HA) antibody (clone 3F10, rat $IgG_1$, Roche Diagnostics, Basel, Switzerland, http://www.roche-applied-science.com) was done using IntraPrep (Immunotech, Marseillu, France, http://www.beckmancoulter.com/products/pr_immunology.asp). Two-color staining with PE-conjugated tetramer of H-$2K^b$-$OVA_{257-264}$-complex (MBL, Nagoya, Japan; http://www.mbl.co.jp/e/index.html) in combination with FITC-conjugated anti-CD8 (clone KT15, Beckman-Coulter) was done according to the manufacturer's instructions.

### Mixed Lymphocyte Reaction

Splenic T-cells were isolated from female C57BL/6 mice by using a pan-T-cell isolation kit (Miltenyi Biotec, Belgish-Bladbach, Germany, http://www.miltenyibiotec.com) and then they were used as responders. Graded numbers of stimulator cells were X-ray irradiated (35 Gy) and cocultured with responders ($1.5 \times 10^5$) in wells of 96-well round-bottomed culture plates for

4 days. [$^3$H]-methyl-thymidine (247.9 Gbq/mmol) was added (0.037 Mbq per well) during the last 16 hours of the culture. At the end of the culture, the cells were harvested onto glass fiber filters (Wallac, Turku, Finland; http://www.perkinelmer.com) and the incorporation of [$^3$H]-thymidine was measured by scintillation counting.

## Antigen Presentation Assay

iPS-DCs were seeded into 96-well flat-bottomed culture plates (1 $\times$ $10^4$ cells per well) with indicated concentrations of OVA protein, IL-4 (10 ng/ml), and anti-CD40 mAb (10 $\mu$g/ml) and cultured overnight. Subsequently, DO11.10 hybridoma cells were added to the wells (5 $\times$ $10^4$ cells per well) and the culture was continued for further 24 hours. At the end of the culture, the concentration of IL-2 in the culture supernatant was measured by ELISA (eBioscience). For the assay with OVA-transfectant iPS-DCs, the indicated numbers of iPS-DCs were cocultured with hybridoma cells, DO11.10 or RF33.70, in the absence of exogenously added antigen for 24 hours and production of IL-2 was also measured by ELISA.

## Analysis of the Activation of NKT Cells by iPS-DCs Loaded with α-Galactosylceramide

Splenic T-cells of (C57BL/6 $\times$ BALB/c) F1 (CBF1) mice were isolated using nylon-wool columns. Mature iPS-DCs were cultured in the presence of α-galactosylceramide (α-GalCer; 100 ng/ml) or vehicle (0.00025% Polysorbate-20) alone for 18 hours, washed, and cocultured with splenic T-cells (1.6 $\times$ $10^5$ DCs + 4 $\times$ $10^6$ T-cells per well in 24-well culture plates). After 24 hours, the cells were recovered and analyzed on their cytotoxic activity by a 4-hour $^{51}$Cr-release assay using YAC-1 cells (5 $\times$ $10^3$ cells per well) as targets in 96-well round-bottomed culture plates. In the analysis of the stimulation of NKT cells in vivo, iPS-DCs loaded with either α-GalCer or vehicle alone were intraperitoneally injected into H-2-matched CBF1 mice (1.2 $\times$ $10^6$ cells per mouse). After 24 hours, the mice were sacrificed and the cytotoxic activity of whole spleen cells pooled from three mice for each group were analyzed using YAC-1 cells as targets, as described earlier.

## Quantitation of Cytokine Production by iPS-DCs

iPS-DCs were cultured in 48-well culture plates (1.5 $\times$ $10^5$ cells/200 $\mu$l per well) in the presence or absence of IL-4 (10 ng/ml), anti-CD40 mAb (10 $\mu$g/ml), TNF-α (10 ng/ml), LPS (1 $\mu$g/ml), and OPK432 (5 or 25 $\mu$g/ml). After 3 days of culture, culture supernatant was collected and concentration of IL-12p70 and TNF-α was determined by using ELISA kits (eBioscience).

## cDNA Microarray Analysis

iPS cell-derived cells in culture step 2, iPS-DCs, iPS-MP, BM-DCs, and BM-MP were recovered from the culture and subjected to cDNA microarray analysis, without purification of specific cell fractions. Total cellular RNA was extracted by using an RNeasy kit (Qiagen, Hilden, Germany, http://www1.qiagen.com). Integrity of RNA samples was verified by using Agilent 2100 Bioanalyzer (Agilent Technologies, Palo Alto, CA, http://www.agilent.com) and the purity and concentration was checked based on A260/280 (A260/280: 1.98~2.04). For each cell sample, cDNA was synthesized by using MMLV-RT using 300 ng of RNA as template and the cDNA was used as template for synthesis of cyanine-3 (Cy-3)-labeled cRNA by using T7 RNA polymerase. A total of 1.65 $\mu$g each of Cy-3-labeled cRNA was hybridized to a microarray slide (Whole Mouse Genome Oligo Micoarray 4 $\times$ 44K; Agilent Technologies; http://www.home.agilent.com) for 17 hours and washed, according to the manufacturer's instructions (Protocol: One-Color Microarray-based Gene Expression Analysis, version 5.7). The slides were scanned on Agilent DNA Microarray Scanner and data were processed and normalized using the GeneSpring GX9.0 software program.

## Plasmid Construction

A cDNA fragment coding for a truncated form of ovalbumin, $OVA_{241-340}$, was prepared by PCR amplification using full length cDNA for OVA as a template with PCR primers 5′-*cctcgag*cccgccgccaccatg*gctagc*atgttggtgctgttgcctgat-3′ (Xho I and Nhe I sites are indicated by underline) and 5′-cttaagcgtagtctgggacgtcgtatgggtactctctgcctgcttcattgatttc-3′. The design of these primers results in the cloning of OVA downstream of the Kozak sequence and the addition of the HA epitope (MYPYDVPDYA) to the carboxyl terminus of OVA fragment. The cDNA fragment for $OVA_{241-340}$-HA was cloned into pCAG-INeo, a mammalian expression vector driven by a CAG promoter and containing the internal ribosomal entry site (IRES)-neomycin resistance gene cassette to generate pCAG-OVA-INeo. A cDNA fragment for amino terminal portion of invariant chain ($Ii_{1-80}$) was prepared by PCR amplification using full-length cDNA for human Ii as a template with PCR primers, 5′-ac*ctcgag*cccgccgccaccatggatgaccagcgcgacctatctc-3′ and 5′-aa*gctagc*aagcttcatgcgcaggttctccag-3′, and inserted into the Xho I-Nhe I site of pCAG-OVA-INeo to generate the Ii-$OVA_{241-340}$ expression vector, pCAG-Ii-OVA-INeo.

## Transfection of iPS Cells by Electroporation

iPS cells maintained on layers of PEF were harvested by using trypsin/EDTA and suspended in DMEM (3 $\times$ $10^7$ cells per milliliter) and 1.2 $\times$ $10^7$ cells were electroporated in a 4-mm-gap cuvette under 225 V and 600 $\mu$F with 30 $\mu$g of plasmid DNA. After electroporation, cells were cultured on neomycin-resistant PEF feeder layers in 100-mm culture dishes in the presence of G418 (500 $\mu$g/ml) for 9–10 days. Subsequently, drug-resistant colonies were picked up and transferred into 24-well culture plates. iPS cell transfectant clones with high levels of expression of the transgene were selected based on the resistance to high-dose (3 mg/ml) of G418. Thereafter, the expression of the transgene after differentiation of the transfectants was examined by intracellular staining with anti-HA mAb and flow cytometric analysis.

## Analysis of In Vivo Priming of Antigen-Specific T-Cells by iPS-DCs

Transfectant or nontransfectant iPS-DCs were stimulated with IL-4, TNF-α, and anti-CD40 mAb and injected intraperitoneally into C57BL/6 mice (1.5 $\times$ $10^5$ cells per mouse). Eight days after the injection, spleen cells were isolated from the injected mice and pooled for each group of three mice. After hemolysis, spleen cells were cultured in 24-well culture plates (3 $\times$ $10^6$ cells/2 ml per well) in RPMI-1640 supplemented with horse serum (10%), recombinant human IL-2 (100 U/ml), and $OVA_{257-264}$ peptide (0.001 $\mu$M). After 5 days, the cells were harvested and OVA-specific cytotoxic T lymphocyte (CTL) activity was analyzed by 5 hour-$^{51}$Cr-releasae assay using OVA-peptide-pulsed or unpulsed EL-4 cells as targets. The percentage of specific lysis was calculated as: 100 $\times$ (experimental release − spontaneous release)/(maximal release − spontaneous release). Spontaneous release and maximal release were determined in the presence of medium or 1% Triton X-100, respectively. The experiments using mice were done according to the plan approved by animal research committee of Kumamoto University. The frequency $CD8^+$ T-cells specific to $OVA_{257-264}$ was analyzed using the PE-labeled tetramer of $K^b$-$OVA_{257-264}$-complex as described earlier.

## Tumor Challenge Experiments

OVA-transfectant or nontransfectant iPS-DCs were injected intraperitoneally into C57BL/6 mice (1.0 $\times$ $10^5$ cells per mouse) on day-10, and MO4 cells (2 $\times$ or 3 $\times$ $10^5$ cells per mouse) were inoculated subcutaneously into the shaved right flank region on day 0. The tumor size was measured on days 11, 15, and 18 and the tumor volume was calculated as follows: tumor volume ($mm^3$) = (length $\times$ width $\times$ height).

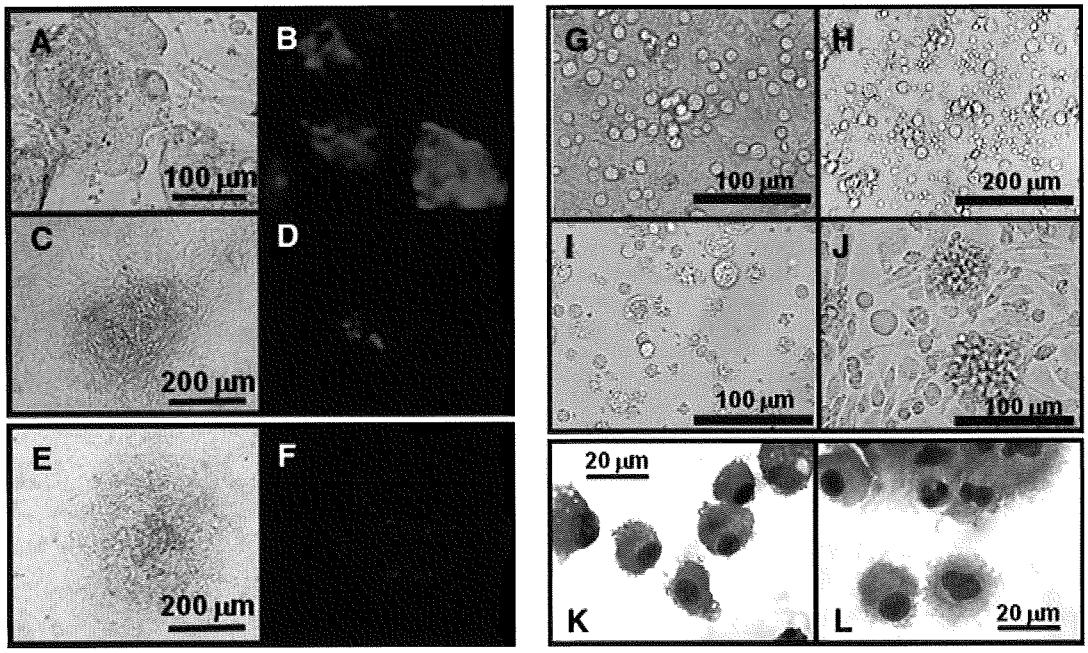


**Figure 1.** Morphological changes from iPS cells to iPS-DC. Phase-contrast images (**A, C**) and fluorescence images showing expression of green fluorescence protein (**B, D**) of undifferentiated Nanog-iPS cell colonies on primary embryonic fibroblasts feeder layer (**A, B**) and a differentiating colony on OP9 feeder layer at day 3 of the step 1 culture (**C, D**). A phase-contrast image (**E**) and a fluorescence image showing expression of Flk-1 (**F**) of a colony at day 6 of the step 1 culture. Phase-contrast images of iPS cell-derived hematopoietic cells at day 3 (**G**) and day 6 (**H**) in step 2 and day 15 (**I, J**) in step 3 are shown. (**K, L**): Cytospin specimens of iPS-DC recovered from step 3 culture were stained with May-Grünwald-Giemsa. Cells in (**I–L**) had been stimulated for 2–4 days with IL-4, TNF-α, and anti-CD40 mAb.

### Chemotaxis Assay

A multiwell chemotaxis assay was done by using 24-well Transwell permeable support chamber (pore size 5 μm; Corning, NY; http://www.corning.com/index.aspx). Cell suspensions ($1 \times 10^6$ cells per ml) in serum-free culture medium (AIMV, Gibco-Invitrogen) were added to the upper compartments (0.1 ml per well) and the indicated concentration of C5a in AIMV medium was added to the lower compartments (0.6 ml per well). Assay plates were incubated at 37°C for 90 minutes and then the cells on the upper surface of the microporous membranes were removed by using swabs. Subsequently, the membranes were fixed with methanol for 5 minutes and stained with May-Giemsa solution (Muto Chemicals, Tokyo, Japan). The stained cells on the lower surface of the membranes were counted and the data were indicated as the number of cells per 1 $mm^2$.

### Phagocytosis Assay

The cell suspensions in RPMI-1640/10% FCS/2-ME were added to 48-well culture plates ($2 \times 10^5$ cells/200 μL per well) and incubated at 37°C for 2 hours to allow the cells to adhere to the plates. FITC-labeled Zymosan A particles (Molecular Probes Inc., Eugene, OR, http://probes.invitrogen.com) were added to the wells ($4.8 \times 10^6$ particles/200 μL per well) and, after incubation for the indicated period, cells were rinsed with PBS and harvested by using trypsin/EDTA. The cells were treated with trypan blue to quench FITC of the cell-surface attached particles, washed and then analyzed on FACScan flow cytometer.

### Measurement of Nitric Oxide Production

The cells suspended in phenol-red-free DMEM/5% FCS were seeded into 96-well plates ($1 \times 10^5$ cells/0.2 ml per well) in the presence or absence of IFN-γ (200 U/ml) and LPS (100 ng/ml). After 24 hours of incubation, concentration of $NO_2 + NO_3$ in the culture supernatant was determined based on Griess method by using a nitric oxide assay kit (Dojindo, Kumamoto, Japan; http://www.dojindo.com).

## Results

### Generation of DCs From iPS Cells

The present study mainly examined iPS-MEF-Ng-38C-2 (38C-2), one of the previously established mouse iPS cell clones [14], for the capacity to differentiate into functional DCs. 38C-2 was developed by introduction of the four genes (Oct3/4, Sox2, Klf4, and c-Myc) for reprogramming factors into embryonic fibroblasts and subsequent selection based on the expression of the Nanog gene. The procedure to induce the differentiation of iPS cells into DCs, composed of three steps as shown in supporting information Figure 1, was basically the same as that developed previously using mouse ES cells [2].

Undifferentiated iPS cells were maintained on the feeder layers of PEF. They were similar to ES cells in morphology (Fig. 1A) and growth properties. Nanog-selected iPS cells carry a transgene of the Nanog genome inserted with a cDNA coding for green fluorescence protein (GFP) in the 5′-untranslated region. The expression of GFP was observed in approximately half of the undifferentiated Nanog-iPS cells (Fig. 1B), as reported previously [14]. To initiate the differentiation, iPS cells were transferred onto OP9 feeder layers (step 1). After 3 days, mesodermally differentiated flat colonies appeared. The expression of GFP was scarcely observed in the differentiated colonies (Fig. 1C, 1D), thus indicating that the promoter of Nanog gene was turned off along with the mesodermal differentiation of iPS cells. On day 6, most of the colonies exhibited a differentiated morphology. They were completely negative for the expression of GFP and positive for cell surface expression of Flk-1/VEGFR2 (Fig. 1E, 1F).

On day 6 or 7 of step 1, cells were harvested by using trypsin/EDTA and dissociated into single cells. Subsequently,

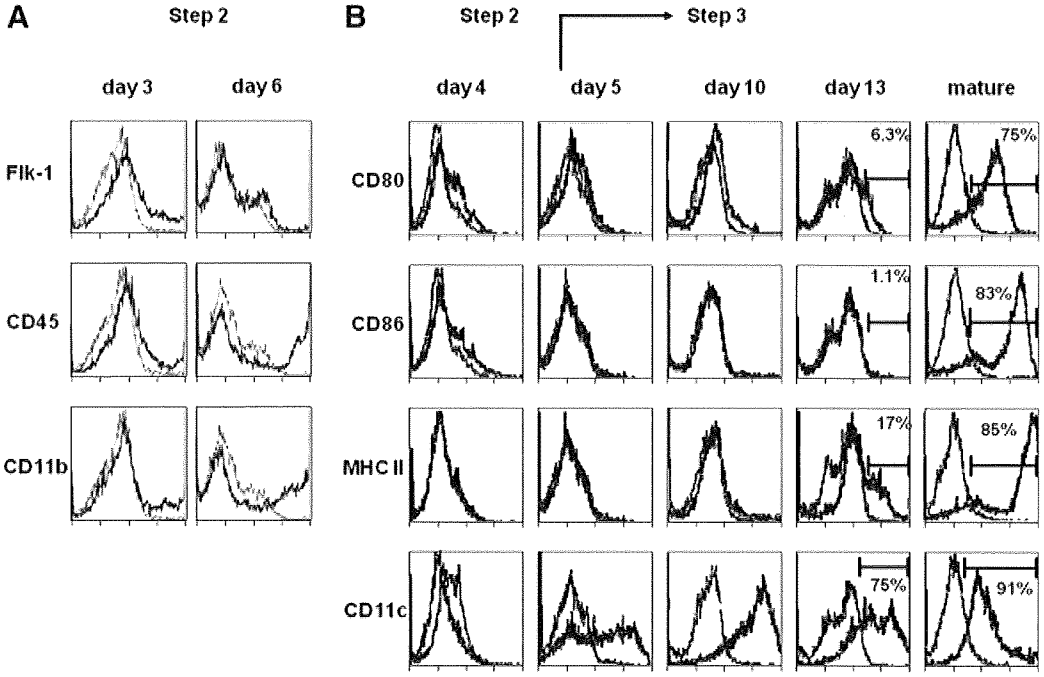


**Figure 2.** Surface phenotypes of iPS-derived cells in differentiation culture. (**A**): The cells at days 3 and 6 in step 2 culture were examined for the expression of Flk-1, CD45, and CD11b. (**B**): The cells in step 2 and step 3 culture were examined for the expression of CD80, CD86, MHC class II, and CD11c. The staining patterns of specific antibodies (thick lines) and isotype-matched controls (thin lines) are shown. The numbers in the panels of day13 and mature DC indicate percentages of cells positive for CD80, CD86, or MHC class II.

the cells were transferred onto freshly prepared OP9 feeder layers and cultured in the presence of GM-CSF, to start step 2. On the next day, homogenous small cells, resembling primitive hematopoietic progenitor cells, appeared (Fig. 1G). The iPS cell-derived round cells, expressing Flk-1 and CD45 (Fig. 2A), gradually increased and became morphologically heterologous (Fig. 1H). The addition of exogenous GM-CSF was essential for the propagation of the cells, thus indicating that the cells proliferated in response to GM-CSF. At day 6 in culture step 2, more than half of the floating cells highly expressed CD11b (Fig. 2A), thus suggesting their commitment to myeloid cell lineage. Step 2 culture was continued for 6–7 days.

At the end of step 2, floating or loosely adherent cells were recovered by pipetting and transferred them into bacteriological Petri dishes without feeder cells (step 3). After 5–7 days, most of floating cells showed irregular shape with some protrusions (supporting information Fig. 2). In addition, some of the transferred cells adhered to the dish surfaces like macrophages. Based on the morphology, the floating cells with protrusions were named iPS-DCs (iPS cell-derived dendritic cells). iPS-DCs expressed CD11c, but did not express CD80, CD86, and MHC class II until day 10 of the step 3 culture (Fig. 2B). At day 13, some of them expressed CD80 and MHC class II, thus suggesting spontaneous partial maturation. After day 10 of the step 3 culture, 1–2 $\times$ $10^6$ iPS-DCs were recovered from one Petri dish. The number of cells increased about 400–600 times from the initiation of the differentiation until differentiation into iPS-DCs.

To induce full maturation of iPS-DCs, we transferred the floating cells into new Petri dishes, and added IL-4, TNF-$\alpha$, and anti-CD40 mAb to the cells simultaneously. In 2 or 3 days, most of the cells exhibited morphology of typical mature DCs, with many long protrusions or veil-like protrusions and some of the cells formed clusters (Fig. 1I–1L). Flow cytometric analysis demonstrated that high levels of cell-surface expression of CD80, CD86, and MHC class II in the mature iPS-DCs (Fig. 2B).

One of the Fbx15-selected iPS cell clones, iPS-MEF-FB-20A-10[13] (20A-10), was also subjected to the differentiation culture. The 20A-10 iPS cells differentiated and proliferated well in the culture steps 1 and step 2, resulting in appearance of a large number of myeloid lineage cells at the end of step 2 (supporting information Fig. 3A). In the step 3 culture with GM-CSF intended for generation of DCs, 20A-10-derived myeloid cells further grew, exhibited some protrusions, and expressed CD11c. However, they were refractory to maturation. Even when stimulated with the simultaneous addition of IL-4, TNF-$\alpha$ and anti-CD40 mAb, they expressed very low level of cell-surface MHC class II and did not express CD80 and CD86 (supporting information Fig. 3B).

## Functions and Gene-Expression of iPS-DCs

Nanog-selected iPS cells including the clone 38C-2 were derived from PEF with a mixed genetic background composed of 75% DBA (H-$2^d$), 12.5% C57BL/6 (H-$2^b$), and 12.5% 129S4 (H-$2^b$) [14], and thus their H-2 haplotype could be b/b, b/d, or d/d. Before the analyses of the immunological functions of iPS-DCs, we determined the H-2 haplotype of 38C-2 iPS cells by flow cytometric and PCR-based analyses and that was found to be d/b (supporting information Fig. 4).

To examine the capacity of iPS-DCs to stimulate T-cells, allogeneic mixed lymphocyte reaction (MLR) assay was conducted using iPS cell-derived cells of several different differentiation stages as stimulators. We used splenic T-cells isolated from naive C57BL/6 mice (H-$2^b$) as allogeneic responder T-cells. As shown in Figure 3A, the floating cells harvested from step 2 culture (pre-iPS-DCs) or at day 8 of step 3 (immature iPS-DCs) exhibited either no or a very low level of activity to stimulate naive T-cells. Partially maturated iPS-DCs harvested on day 15 of the step 3 culture induced a small but definite proliferative response of T-cells. In contrast,

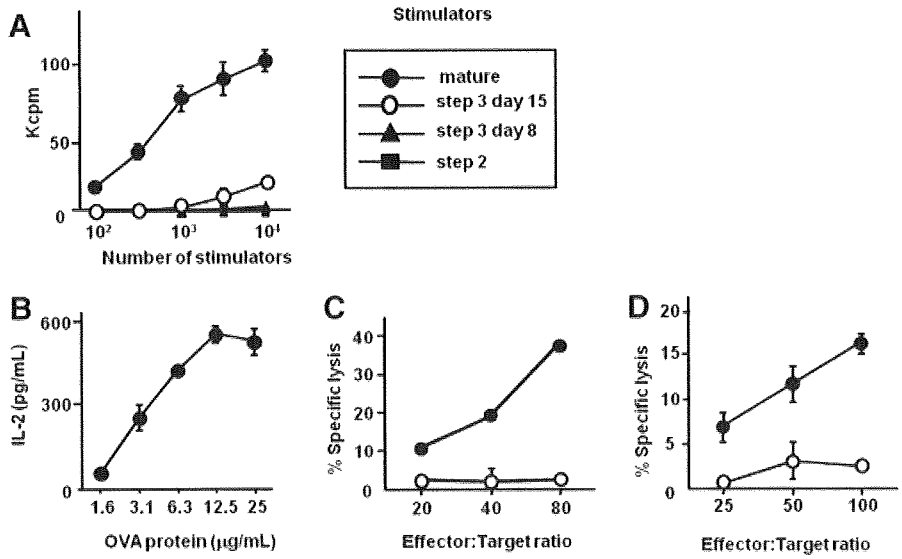


**Figure 3.** Antigen-processing and presenting function of iPS-DC in vitro. (**A**): Pre-iPS-DC harvested from step 2 culture, immature iPS-DC (day 8 of step 3), partially maturated iPS-DC (day 15 of step 3) and fully maturated iPS-DC were cocultured with T-cells from C57BL/6 mice in wells of 96-well round-bottomed plates and cultured for 4 days. Proliferation of the T-cells was measured based on the incorporation of [$^3$H]-thymidine. (**B**): iPS-DC were cultured in 96-well flat-bottomed culture plates in the presence of indicated concentrations of ovalbumin protein, IL-4, and anti-CD40 mAb for overnight. Subsequently, T-cell-hybridoma cells (DO11.10) were added and further cultured for 24 hours. The concentration of IL-2 produced by the hybridoma in the culture supernatant was measured by ELISA. (**C**): Mature iPS-DC were loaded with either α-GalCer (closed symbols) or vehicle alone (open symbols) for 18 hours, washed and cocultured with splenic T-cells of H-2-matched (C57BL/6 × BALB/c) F1 (CBF1) mice. After 24 hours of culture, cytotoxic activity of the cultured cells against YAC-1 cells were analyzed by 4-hour Cr-release assay. (**D**): iPS-DC were loaded with either α-GalCer (closed symbols) or vehicle alone (open symbols) as in (**C**) and intraperitoneally injected into CBF1 mice ($1.2 \times 10^6$ cells per mouse). After 24 hours, spleen cells isolated from the three mice for each group were pooled and their cytotoxic activity against YAC-1 cells were analyzed by 4-hour Cr-release assay. Abbreviation: Kcpm, kilo counts per minute.

iPS-DCs treated with maturation stimuli for 2 days exhibited a very high magnitude of T-cell-stimulating activity (Fig. 3A), consistent with their high levels of cell-surface expression of MHC class II and costimulatory molecules (Fig. 2B).

To examine the antigen-processing and presentation function of iPS-DCs, the presentation of OVA antigen to a T-cell hybridoma, DO11.10, recognizing $OVA_{323-339}$ in the context of I-$A^d$, was analyzed. iPS-DCs harvested at day 10-day of culture step 3 were cultured in the presence of OVA protein, IL-4 and anti-CD40 mAb in 96-well culture plates, to allow them to capture the antigenic protein and to maturate. After 18 hours, DO11.10 hybridoma cells were added and then were further cultured. In this assay, IL-2 in the culture supernatant produced by DO 11.10 indicated the presentation of OVA-derived epitope on the I-$A^d$ of iPS-DCs. The results shown in Figure 3B indicate that DO11.10 produced IL-2 depending on the concentration of OVA protein loaded to iPS-DCs, thus demonstrating processing of the antigenic protein and presentation of the I-$A^d$-restricted epitope by iPS-DCs.

NKT cells are a group of T-cells expressing invariant T-cell receptors and recognize lipid ligands, for example α-GalCer, in the context of CD1d, a nonclassical MHC class I. On simulation with α-GalCer, NKT cells rapidly produce large amount of cytokines, resulting in activation of conventional T-cells and NK cells. α-GalCer-loaded DCs are known to be efficient in activation of NKT cells [7, 28–30]. We also analyzed the capacity to present α-GalCer and activate NKT cells. Mature iPS-DCs were loaded with α-GalCer or vehicle alone and cocultured with H-2-matched splenic T-cells from (C57BL/6 × BALB/c) F1 (CBF1) mice (H-$2^{b/d}$) for 24 hours. As shown in Figure 3C, the cells cocultured with α-GalCer-loaded iPS-DCs but not those cultured with vehicle-loaded iPS-DCs exhibited activity to kill YAC-1 cells, indicating activation of NKT cells by α-GalCer-loaded iPS-DCs. To examine the in vivo stimulation of NKT cells, iPS-DCs loaded with either α-GalCer or vehicle alone were intraperitoneally injected into CBF1 mice. Spleen cells isolated from the mice injected with α-GalCer-loaded iPS-DCs showed higher cytotoxic activity against YAC-1 cells than those from mice injected with vehicle-loaded iPS-DCs (Fig. 3D), thus demonstrating in vivo activation of NKT cells by α-GalCer-loaded iPS-DCs.

To know how long iPS-DCs could survive in vivo, we injected carboxyfluorescein succinimidyl ester (CFSE)-labeled iPS-DCs ($2 \times 10^6$ per mouse) into H-2-matched CBF1 mice at the tail-base and analyzed the frequency of CFSE-positive cells in the draining para-aortic lymph nodes after 3, 5, 8, 14, and 21 days (supporting information Fig. 5). As a result, we observed that injected iPS-DCs survived more than 14 days in the draining lymph nodes.

Next, the production of IL-12 and TNF-α by iPS-DCs upon treatment with stimulatory ligands was analyzed (Fig. 4A, 4B). The addition of IL-4 and anti-CD40 mAb exhibited little effect to enhance the production of IL-12p70. The addition of either LPS or OK432 but not TNF-α significantly enhanced the production of IL-12. The addition of LPS and OK432 exhibited dramatic effect to enhance the production of TNF-α. Collectively, the production of IL-12 and TNF-α by iPS-DCs was significantly enhanced on stimulation with bacteria-derived stimulatory ligands, similarly as the case of physiological DCs.

The global gene-expression profile of iPS-DCs was examined by using DNA microarrays. As shown in Figure 4C, the gene expression profile of iPS-DCs was similar to that of BM-DCs. We analyzed the change of gene expression profile during the step 3 culture, by comparing the data of cells recovered at the end of step 2 and those of iPS-DCs (Fig.

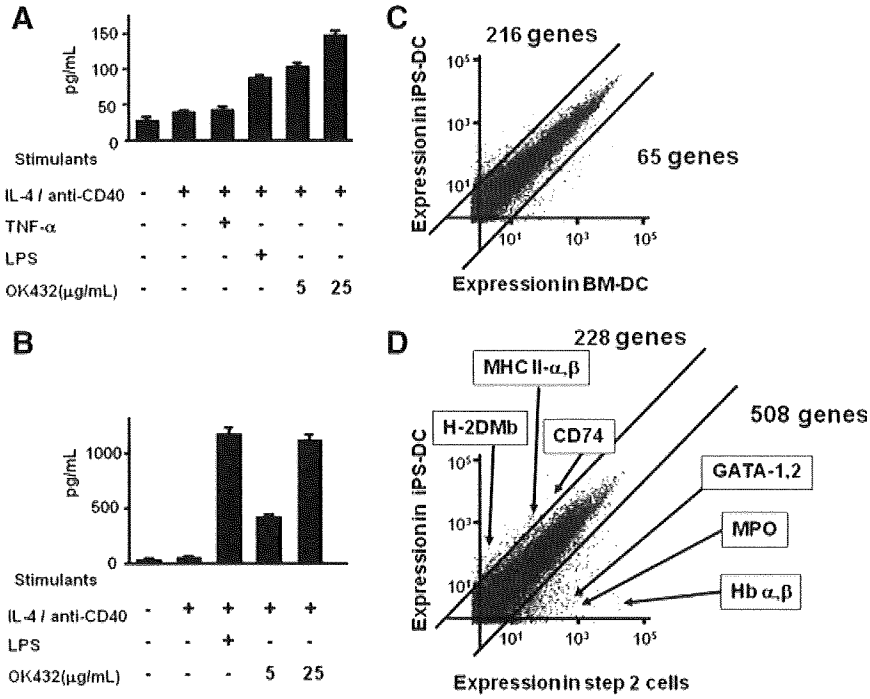


**Figure 4.** Cytokine production and gene-expression profiles of iPS-DC. (**A, B**): iPS-DC were cultured in the presence or absence of IL-4 (10 ng/ml), anti-CD40 mAb (10 μg/ml), TNF-α (10 ng/ml), LPS (1 μg/ml), and OK432 (5 or 25 μg/ml) as indicated. After 3 days of culture, culture supernatant was collected and concentration of IL-12p70 (**A**) and TNF-α (**B**) was determined by ELISA. (**C**): A scattered plot comparing global gene-expression profiles of BM-DC and iPS-DC. The numbers of more than 10-fold differentially expressed genes among the total of 22,506 genes (array spots) analyzed are shown. The results of flow cytometric analysis of iPS-DC and BM-DC are shown in Figure 1A (step 3, day 13) and supporting information Figure 6, respectively. (**D**): A scattered plot comparing gene-expression profiles of step 2 culture cells (pre-iPS-DC) and iPS-DC. The levels of expression of genes for H-2DMβ (H-2DMb), MHC class II α and β, MHC class II-associated invariant chain (Ii/CD74), GATA-1, GATA-2, MPO, and hemoglobin (Hb) α and β are indicated. Among the total of 23,481 genes (array spots) analyzed, the number of genes with more than 10-fold increase or decrease in the level of expression is shown. The results of flow cytometric analysis of step 2 cells are shown in Figure 1A (step 2, day 6). Abbreviations: LPS, lipopolysaccharide; MPO, myeloperoxidase; TNF, tumor necrosis factor.

4D). The results showed that 228 out of 23,481 analyzed genes were upregulated more than 10 times (listed in supporting information Table 1) and such dramatically upregulated genes included those directly associated with antigen-presenting functions (Fig. 4D), such as MHC class II, CD74, and H2-DM. On the other hand, a number of genes were expressed highly in the step 2 cells and at very levels in iPS-DCs, for example hemoglobin α and β chains, myeloperoxidase (MPO), GATA-1, and GATA-2 genes (Fig. 4D). These down-modulated genes were probably expressed by erythroid and myeloid precursor cells included in the cells of step 2 which disappeared along with differentiation into iPS-DCs in the step 3 culture.

## Genetic Modification of iPS-DCs

Genetic modification is a valuable means for modifying the function of DCs for medical application. For example, by means of the forced expression of antigenic proteins and immunostimulatory molecules, we can generate DCs vaccines potently inducing immune response to specific antigens [6]. In the present study, we generated an expression vector from which a model antigen, OVA protein, was expressed as a fusion protein with MHC class II-associated invariant chain (Ii). Ii-fused OVA protein (Ii-OVA) produced in the APC was expected to be transported to endosomes and digested and thus epitopes derived from this protein could be presented in the context of MHC class II, in addition to MHC class I.

As shown in Figure 5A, the expression vector for Ii-OVA was created by ligating the cDNA fragment encoding for aminoterminal portion of Ii (p1-81), including an endosome targeting signal sequence (di-leucin motif), with that encoding for a truncated form of OVA protein ($OVA_{241-340}$) attached with an HA-tag. 38C-2 iPS cells were introduced with the vector and selected by culture in the presence of G418 and then 48 transfectant iPS cell clones were isolated. The expression of the transgene after differentiation to iPS-DCs was detected by flow cytometric analysis following intracellular staining with anti-HA mAb. The results of flow cytometric analysis of the parental 38C-2 iPS cell-derived DCs (nontransfectant iPS-DCs) and the Ii-OVA-transfectant iPS-DCs (iPS-DCs/OVA) are shown in Figure 5B and 5C, respectively.

iPS-DCs/OVA were examined for the presentation of OVA-derived epitopes in the context of MHC class I and MHC class II molecules. iPS-DCs/OVA or nontransfectant iPS-DCs were cocultured with T-cell hybridomas, RF33.70 (recognizing $OVA_{257-264}$ in the context of H-$2K^b$) and DO11.10 (recognizing $OVA_{323-339}$ in the context of I-$A^d$). As shown in Figure 5D and 5E, iPS-DCs/OVA stimulated both of the T-cell hybridomas to produce IL-2, whereas nontransfectant iPS-DCs did not. Collectively, we verified the expression by iPS-DCs of transgene introduced before differentiation and confirmed that iPS-DCs possess a physiological intracellular antigen presentation machinery.

## Priming of Antigen-Specific Cytotoxic T-Cells In Vivo by Genetically Modified iPS-DCs

To analyze the capacity of iPS-DCs/OVA to prime OVA-specific T-cells in vivo, we injected iPS-DCs/OVA or nontransfectant iPS-DCs intraperitoneally into C57BL/6 mice. In this experiment, injected iPS-DCs were derived from 38C-2 iPS

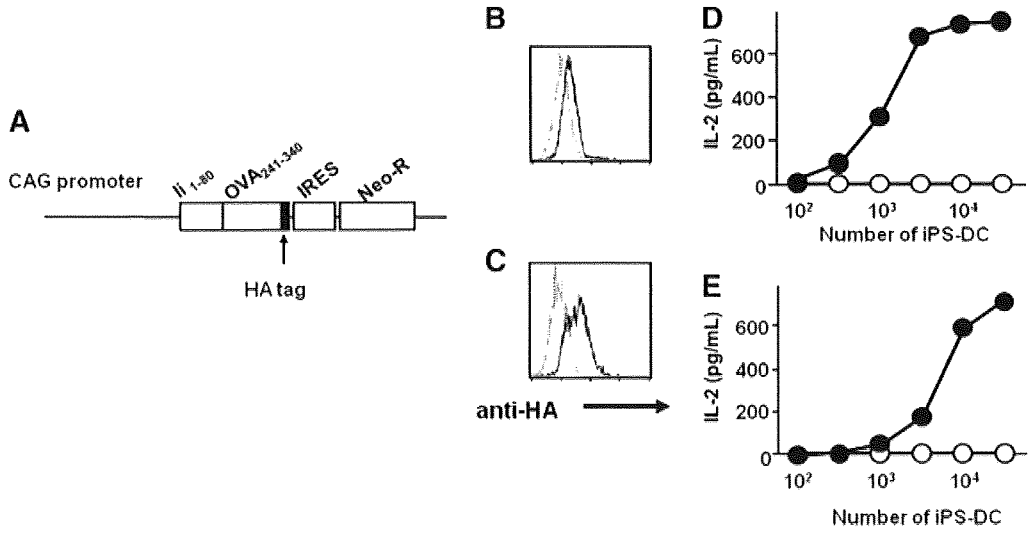


**Figure 5.** Genetic modification of iPS-DC to express antigenic protein. (**A**): The structure of pCAG-IiOV, an expression vector for Ii-OVA chimeric protein attached with HA-Tag. (**B, C**): Nontransfectant iPS-DC (**B**) or Ii-OVA transfectant iPS-DC (**C**) were stained intracellularly with FITC-conjugated anti-HA mAb (thick lines) or left unstained (thin dotted lines) and analyzed by flow cytometry. (**D, E**): Nontransfectant iPS-DC (open symbols) or Ii-OVA transfectant iPS-DC (closed symbols) were cocultured with T-cell hybridomas, RF33.70 (**D**, recognizing $OVA_{257-264}$ in the context of $K^b$) or DO11.10 (**E**, recognizing recognizing$OVA_{323-339}$ in the context of $I\text{-}A^d$). Abbreviations: HA, hemagglutinin; IRES, internal ribosomal entry site.

cells ($H\text{-}2^{b/d}$) and the recipient mice were of C57BL/6 strain ($H\text{-}2^{b/b}$). Therefore, iPS-DCs were semiallogeneic to the recipient mice sharing $H\text{-}2^b$-haplotype with the recipient. This experimental design was based on our previous observation that ES-DCs could prime antigen-specific CTL restricted to the MHC molecule of the shared allele in such semiallogeneic recipient mice [8, 10]. Eight days after the injection, splenocytes were isolated from the mice and cultured in the presence of $OVA_{257-264}$ peptide, the major $H\text{-}2K^b$-restricted epitope derived from OVA protein. After 5 days, cultured cells were recovered and examined for the frequency and cytotoxic activity of $H\text{-}2K^b\text{-}OVA_{257-264}$-specific $CD8^+$ T-cells (Fig. 5A).

The results showed that 1.56% of the $CD8^+$ T-cells in the cultured spleen cells isolated from the mice injected with iPS-DCs/OVA were positively stained with tetramer of $K^b\text{-}OVA_{257-264}$-complex (Fig. 5B). On the other hand, these were 0.22% in the cells from the mice injected with nontransfectant iPS-DCs (Fig. 5C). The results shown in Figure 5D indicated that cytotoxic T-cells specific to the OVA epitope was primed in vivo by iPS-DCs/OVA but not by nontransfectant iPS-DCs. These results demonstrate that iPS-DCs genetically engineered to express an antigenic protein primed cytotoxic T-cells specific to the antigen upon in vivo administration.

We examined whether antigen-specific anti-tumor immunity was induced by iPS-DCs expressing antigenic protein or not. Ten days after the intraperitoneal injection of iPS-DCs/OVA or nontransfectant iPS-DCs, the recipient C57BL/6 mice were challenged by subcutaneous injection of MO4, an OVA expressing melanoma cell line derived from a C57BL/6 mouse. As shown in Figure 6E, the growth of tumor in the mice was almost completely inhibited by pretreatment with iPS-DCs/OVA but not by nontransfectant ES-DCs. Therefore, it was demonstrated that in vivo transfer of genetically modified iPS-DCs expressing model tumor antigen efficiently induced antigen-specific anti-tumor immunity.

## Generation of Macrophages From iPS Cells

As described earlier, in the step 3 of iPS-DCs differentiation culture, some adherent cells were observed and they showed macrophage-like morphology. To promote the differentiation into macrophages, M-CSF was added instead of GM-CSF in the step 3 culture. As a result, a large number of macrophage-like adherent cells appeared from 38C-2 (Nanog-selected) iPS cells (Fig. 7A, 7B). These were designated as iPS-MP (iPS cell-derived macrophages). The iPS-MP were harvested by treatment with trypsin/EDTA and then were characterized.

A flow cytometric analysis shown in Figure 7C revealed that iPS-MP expressed F4/80 and CD11b, as macrophages generated from bone marrow cells (BM-MP) did. The level of expression of CD14 in iPS-MP was very low. iPS-MP showed C5a-induced chemotaxis (Fig. 7D). Their phagocytic capacity was assessed by using FITC-labeled zymosan particles. As shown in Figure 7E, iPS-MP ingested zymosan particles in a similar rate as BM-MP did. Stimulation with LPS and IFN-$\gamma$ synergistically induced production of nitric oxide by iPS-MP (Fig. 7F).

Consistent with the results of the functional analysis, gene expression profile of iPS-MP revealed by cDNA microarray analysis was relatively similar to that of BM-MP (Fig. 7G). In the analysis of change of gene expression from precursor cells (recovered from step 2 culture) to iPS-MP (Fig. 7H), we found that the expression of some genes associated with function of macrophages was drastically increased. For example, expression of CD14, Msr (macrophage scavenger receptor) two, and CD36 were upregulated more than 20 times during the iPS-MP differentiation. The 157 genes with more than a 10 time-increase in the level of expression during the differentiation from culture step 2 to iPS-MP were listed in the supporting information Table 2.

Collectively, culture of iPS cell-derived myeloid lineage cells harvested from the culture step 2 in the presence of exogenous M-CSF resulted in the generation of macrophages (iPS-MP). The characteristics of iPS-MP as macrophages were confirmed by their morphology, cell surface phenotypes, functions and also gene-expression profile.

An Fbx15-selected iPS cell clone 20A-10 also showed morphology and cell surface markers of macrophages, when subjected to the differentiation culture for iPS-MP (supporting information Fig. 3C, 3D). Therefore, in the present study,

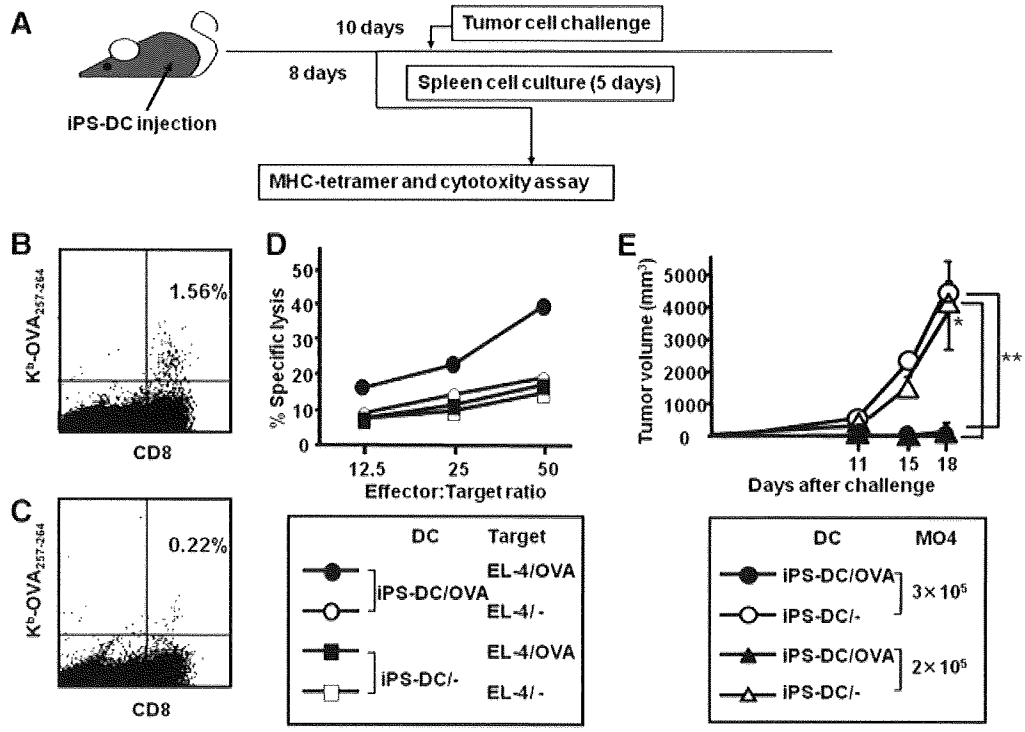


**Figure 6.** Activation of T-cells in vivo by iPS-DC. (**A**): A schematic depiction of the experiment to analyze the priming of antigen-specific T-cells by iPS-DC in vivo. Ii-OVA transfectant iPS-DC (iPS-DC/OVA) or nontransfectant iPS-DC were injected intra-peritoneally into C57BL/6 mice ($1.5 \times 10^5$ cells per mouse). Eight days after the injection, spleen cells were isolated from the mice and cultured in the presence of $OVA_{257-264}$ peptide. After 5 days, cultured cells from iPS-DC/OVA-injected (**B**) or nontransfectant iPS-DC-injected (**C**) were stained with tetramer of H-$2K^b$-$OVA_{257-264}$ in combination with anti-CD8 mAb. (**D**): OVA-specific CTL activity was analyzed by $^{51}Cr$-releasae assay using OVA-peptide-pulsed (closed symbols) or unpulsed (open symbols) EL-4 cells as targets. (**E**): Ten days after the injection of iPS-DC/OVA or non-transfectant iPS-DC into C57BL/6 mice ($1 \times 10^5$ cells per mouse), the mice were subcutaneously injected with MO4, an OVA expressing melanoma cell line, (two × or $3 \times 10^5$ cells per mouse, 5–6 mice per group), at the shaved right flank. After that, the tumor size was measured and the tumor volume was calculated as: tumor volume ($mm^3$) = (length × width × height). *One mouse out of five mice pre-treated with non-tranfectant iPS-DC and challenged with $2 \times 10^5$ MO4 cells died between days 15 and 18. **The results of iPS-DC/OVA-treated and non-transfectant iPS-DC-treated mouse groups were different with statistical significance for both $2 \times 10^5$ and $3 \times 10^5$ MO4 cell-injected groups ($p < .001$ by Student's $t$ test). Abbreviations: DC, dendritic cells; OVA, ovalbumin.

20A-10 iPS cells differentiated into macrophages but not into DCs.

## Discussion

The present study demonstrated that Nanog-selected iPS cells (38C-2) were capable of differentiating into functional DCs and macrophages. The morphological changes observed during the differentiation of the iPS cells into DCs were very similar to that observed in the differentiation culture for ES-DCs [2]. However, there was some delay (1–2 days in step 1 and 2 and 2–4 days in step 3) in the kinetics of differentiation process of iPS cells, as in comparison with most of mouse ES cell lines. On the other hand, the yield of differentiated cells (up to 600 times the cell number from undifferentiated iPS cells to differentiated iPS-DCs) was higher than that in the cases of most of ES cell lines (usually up to 400 times). In contrast to 38C-2 iPS cells, we could generate macrophages but not DCs from 20A-10 (Fbx15-selected) iPS cells.

The difference in the potential of differentiation among ES cells and the two clones of iPS cells might be due to the expression of transgenes for reprogamming factors in iPS cell-derived cells during differentiation. To assess this possibility, we analyzed the expression of the transgene-derived reprogramming factors in iPS cells before and after differentiation by reverse transcription polymerase chain reaction (RT-PCR) (supporting information Fig. 7). The expression of all four transgene-derived reprogramming factors was detected during the culture steps 2 and 3 in 38C-2 (Nanog-selected) iPS cells, although the expression of Klf4 was scarce. As for Fbx15-selected 20A-10 iPS cells, three transgene-derived reprogramming factors other than Oct3/4 were detected during differentiation. Collectively, most of the transgene-derived reprogramming factors were expressed during differentiation in the both of iPS cell clones, and they possibly exerted some influence on the differentiation process. However, the reason for the difference in the differentiation potential between the two iPS cell clones was not clarified by this RT-PCR experiment.

As a means to induce T-cell-mediated anti-cancer immunity, vaccination with DCs loaded with tumor antigen-derived peptides or tumor cell lysates are being clinically tested. For this purpose, human DCs are generated from monocytes obtained from peripheral blood of the patients. However, because monocytes cannot be propagated in vitro, apheresis, a procedure sometimes invasive for the patients, is necessary to obtain sufficient number of monocytes as the source of DCs. iPS cells, like ES cells, possess practically unlimited propagation capacity and may be an ideal source for DCs to be used in such immunotherapy.

Embryoid body-mediated differentiation to generate macrophages from mouse ES cells has been reported by several groups [31–34]. In the present study, we demonstrated

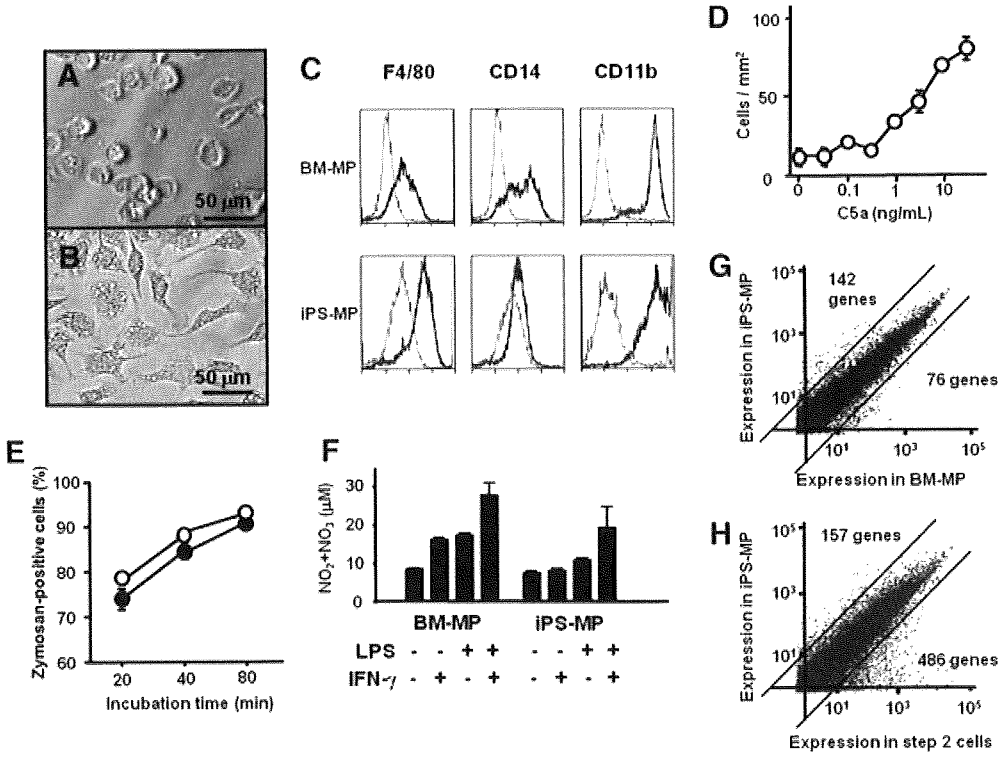


**Figure 7.** Characterization of iPS cell-derived macrophages. Phase-contrast images of iPS-MP in a bacterial Petri dish (**A**) and in a tissue culture-coated dish (**B**) are shown. (**C**): The expression of F4/80, CD14, and CD11b on BM-MP and iPS-MP was analyzed by flow cytometry. (**D**): C5a-induced chemotaxis of iPS-MP was analyzed using 24-well culture plates with permeable membrane insets. (**E**): BM-MP (open circles) or iPS-MP (closed circles) in 48-well culture plates were added with FITC-labeled Zymosan A particles. After incubation for the indicated period, cells were harvested by using trypsin/EDTA, treated with trypan blue, washed and then analyzed on a FACScan. (**F**): Production of nitric oxide by BM-MP and iPS-MP stimulated with IFN-$\gamma$ and/or LPS was analyzed. The cells were seeded onto 24-well culture plates ($1 \times 10^5$ cells/0.2 ml per well) in the presence or absence of the stimulants, as indicated. After 24 hours of incubation, culture supernatant was collected and concentration of $NO_2 + NO_3$ was determined by the Griess method. (**G**): A scattered plot comparing of the gene-expression profiles of BM-MP and iPS-MP is shown. The numbers of more than 10-fold differentially expressed genes among the total of 21,896 genes (array spots) analyzed are shown. The results of flow cytometric analysis of BM-MP and iPS-MP are shown in (**C**). (**H**): A scattered plot comparing the gene-expression profiles of step 2 culture cells and iPS-MP is shown. Among the total of 22,552 genes (array spots) analyzed, the number of genes with more than 10-fold increase or decrease in the level of expression is shown. The results of flow cytometric analysis of step 2 cells are shown in Figure 1A (step 2, day 6). Abbreviation: LPS, lipopolysaccharide.

efficient generation of functional macrophages from mouse iPS cells. Although we had not performed the embryoid body-mediated methods to generate macrophages, the reported ES cell-derived macrophages seemed to be similar to iPS-MP. Physiologically, macrophages play important roles in the defense mechanism against various infectious organisms and also in maintenance of homeostasis by ingestion and digestion of dead cells occurring in the body. The technology to generate large number of functional macrophages from iPS cells may be applicable to the development of novel macrophage-based medical technology.

## Summary

DCs and macrophages were generated by directed in vitro differentiation of mouse iPS cells. The iPS cell-derived DCs (iPS-DCs) possessed the characteristics of DCs including the capacity of T-cell-stimulation, antigen-processing, and presentation and cytokine production. There was some delay in the kinetics of differentiation process of iPS cells, as in comparison with most of mouse ES cell lines. On the other hand, the yield of differentiated cells was higher than that in the cases of most of mouse ES cell lines. Genetically modified iPS-DCs expressing antigenic protein primed T-cells specific to the antigen in vivo. Macrophages generated from iPS cells (IPS-MP) were comparable with bone marrow cell-derived macrophages in the cell surface phenotype, functions, and gene expression profiles.

## Acknowledgments

This work was supported in part by Grants-in-Aid Nos. 18014023, 19591172, and 19059012 from the Ministry of Education, Culture, Sports, Science and Technology (MEXT), Japan, the Program of Founding Research Centers for Emerging and Reemerging Infectious Diseases launched as a project commissioned by MEXT, Japan, Research Grant for Intractable Diseases from Ministry of Health and Welfare, Japan, grants from Japan Science and Technology Agency (JST), the Uehara Memorial Foundation, and the Takeda Science Foundation.

## Disclosure of Potential Conflicts of Interest

The authors indicate no potential conflicts of interest.

## REFERENCES


1 Fairchild PJ, Brook FA, Gardner RL et al. Directed differentiation of dendritic cells from mouse embryonic stem cells. Curr Biol 2000; 10:1515–1518.
2 Senju S, Hirata S, Matsuyoshi H et al. Generation and genetic modification of dendritic cells derived from mouse embryonic stem cells. Blood 2003;101:3501–3508.
3 Zhan X, Dravid G, Ye Z et al. Functional antigen-presenting leucocytes derived from human embryonic stem cells in vitro. Lancet 2004;364:163–171.
4 Slukvin II, Vodyanik MA, Thomson JA et al. Directed differentiation of human embryonic stem cells into functional dendritic cells through the myeloid pathway. J Immunol 2006;176:2924–2932.
5 Senju S, Suemori H, Zembutsu H et al. Genetically manipulated human embryonic stem cell-derived dendritic cells with immune regulatory function. Stem Cells 2007;25:2720–2729.
6 Matsuyoshi H, Senju S, Hirata S et al. Enhanced priming of antigen-specific CTLs in vivo by embryonic stem cell-derived dendritic cells expressing chemokine along with antigenic protein: application to antitumor vaccination. J Immunol 2004;172:776–786.
7 Matsuyoshi H, Hirata S, Yoshitake Y et al. Therapeutic effect of α-galactosylceramide-loaded dendritic cells genetically engineered to express SLC/CCL21 along with tumor antigen against peritoneally disseminated tumor cells. Cancer Sci 2005;96:889–896.
8 Fukuma D, Matsuyoshi H, Hirata S et al. Cancer prevention with semi-allogeneic ES cell-derived dendritic cells. Biochem Biophys Res Commun 2005;335:5–13.
9 Motomura Y, Senju S, Nakatsura T et al. Embryonic stem cell-derived dendritic cells expressing glypican-3, a recently identified oncofetal antigen, induce protective immunity against highly metastatic mouse melanoma, B16-F10. Cancer Res 2006;66:2414–2422.
10 Matsunaga Y, Fukuma D, Hirata S et al. Activation of antigen-specific cytotoxic T lymphocytes by β2-microglobulin or TAP1 gene disruption and the introduction of recipient-matched MHC class I gene in allogeneic embryonic stem cell-derived dendritic cells. J Immunol 2008;181:6635–6643.
11 Hirata S, Senju S, Matsuyoshi H et al. Prevention of experimental autoimmune encephalomyelitis by transfer of embryonic stem cell-derived dendritic cells expressing Myelin oligodendrocyte glycoprotein peptide along with TRAIL or programmed death-1 ligand. J Immunol 2005;174:1888–1897.
12 Hirata S, Matsuyoshi H, Fukuma D et al. Involvement of regulatory T cells in the experimental autoimmune encephalomyelitis-preventive effect of dendritic cells expressing myelin oligodendrocyte glycoprotein plus TRAIL. J Immunol 2007;178:918–925.
13 Takahashi K, Yamanaka S. Induction of pluripotent stem cells from mouse embryonic and adult fibroblast cultures by defined factors. Cell 2006;126:663–676.
14 Okita K, Ichisaka T, Yamanaka S. Generation of germline-competent induced pluripotent stem cells. Nature 2007;448:313–317.
15 Takahashi K, Tanabe K, Ohnuki M et al. Induction of pluripotent stem cells from adult human fibroblasts by defined factors. Cell 2007;131:861–872.
16 Yu J, Vodyanik MA, Smuga-Otto K et al. Induced pluripotent stem cell lines derived from human somatic cells. Science 2007;318:1917–1920.
17 Wernig M, Meissner A, Foreman R et al. In vitro reprogramming of fibroblasts into a pluripotent ES-cell-like state. Nature 2007;448: 318–324.
18 Meissner A, Wernig M, Jaenisch R. Direct reprogramming of genetically unmodified fibroblasts into pluripotent stem cells. Nat Biotechnol 2007;25:1177–1181.
19 Park IH, Zhao R, West JA et al. Reprogramming of human somatic cells to pluripotency with defined factors. Nature 2008;451: 141–146.
20 Lowry WE, Richter L, Yachechko R et al. Generation of human induced pluripotent stem cells from dermal fibroblasts. Proc Natl Acad Sci USA 2008;105:2883–2888.
21 Schenke-Layland K, Rhodes KE, Angelis E et al. Reprogrammed mouse fibroblasts differentiate into cells of the cardiovascular and hematopoietic lineages. Stem Cells 2008;26:1537–1546.
22 Mauritz C, Schwanke K, Reppel M et al. Generation of functional murine cardiac myocytes from induced pluripotent stem cells. Circulation 2008;118:507–517.
23 Narazaki G, Uosaki H, Teranishi M et al. Directed and systematic differentiation of cardiovascular cells from mouse induced pluripotent stem cells. Circulation 2008;118:498–506.
24 Kodama H, Nose M, Niida S et al. Involvement of the c-kit receptor in the adhesion of hematopoietic stem cells to stromal cells. Exp Hematol 1994;22:979–984.
25 Rock KL, Rothstein L, Gamble S. Generation of class I MHC-restricted T-T hybridomas. J Immunol 1990;145:804–811.
26 Haskins K, Kubo R, White J et al. The major histocompatibility complex-restricted antigen receptor on T cells. I. Isolation with a monoclonal antibody. J Exp Med 1983;157:1149–1169.
27 Falo LD Jr., Kovacsovics-Bankowski M, Thompson K et al. Targeting antigen into the phagocytic pathway in vivo induces protective tumour immunity. Nat Med 1995;1;649–653.
28 Kitamura H, Iwakabe K, Yahata T et al. The natural killer T (NKT) cell ligand α-galactosylceramide demonstrates its immunopotentiating effect by inducing interleukin (IL)-12 production by dendritic cells and IL-12 receptor expression on NKT cells. J Exp Med 1999;189: 1121–1128.
29 Toura I, Kawano T, Akutsu Y et al. Cutting edge: Inhibition of experimental tumor metastasis by dendritic cells pulsed with α-galactosylceramide. J Immunol 1999;163:2387–2391.
30 Fujii S, Shimizu K, Kronenberg M et al. Prolonged IFN-γ-producing NKT response induced with α-galactosylceramide-loaded DCs. Nat Immunol 2002;3:867–874.
31 Keller G, Kennedy M, Papayannopoulou T et al. Hematopoietic commitment during embryonic stem cell differentiation in culture. Mol Cell Biol 1993;13:473–486.
32 Moore KJ, Fabunmi RP, Andersson LP et al. In vitro-differentiated embryonic stem cell macrophages: A model system for studying atherosclerosis-associated macrophage functions. Arterioscler Thromb Vasc Biol 1998;18:1647–1654.
33 Lindmark H, Rosengren B, Hurt-Camejo E et al. Gene expression profiling shows that macrophages derived from mouse embryonic stem cells is an improved in vitro model for studies of vascular disease. Exp Cell Res 2004;300:335–344.
34 Odegaard JI, Vats D, Zhang L et al. Quantitative expansion of ES cell-derived myeloid progenitors capable of differentiating into macrophages. J Leukoc Biol 2007;81:711–719.


See www.StemCells.com for supporting information available online.

Immunology Letters 126 (2009) 67–72

Contents lists available at ScienceDirect

Immunology Letters

journal homepage: www.elsevier.com/locate/

# An in vivo model of priming of antigen-specific human CTL by Mo-DC in NOD/Shi-scid IL2rγ$^{null}$ (NOG) mice

Mitsuhiro Inoue[a,b], Satoru Senju[a,c], Shinya Hirata[a], Atsushi Irie[a], Hideo Baba[b], Yasuharu Nishimura[a,*]

[a] Department of Immunogenetics, Graduate School of Medical Sciences, Kumamoto University, Honjo 1-1-1, Kumamoto, 860-8556, Japan
[b] Department of Gastroenterological Surgery, Graduate School of Medical Sciences, Kumamoto University, Honjo 1-1-1, Kumamoto, 860-8556, Japan
[c] Japan Science and Technology Agency, CREST, Tokyo, Japan

ARTICLE INFO

*Article history:*
Received 9 May 2009
Received in revised form 28 July 2009
Accepted 2 August 2009
Available online 12 August 2009

*Keywords:*
NOG mice
NOD/Shi-scid IL2rγ$^{null}$ mouse
Human CTL
Tumor immunity

ABSTRACT

In vivo assay to evaluate anti-cancer immunotherapy at the pre-clinical phase is eagerly needed. We currently established xenotransplantation-based method to analyze in vivo priming of cancer-antigen-specific human cytotoxic T lymphocytes (CTLs). We transplanted human peripheral T cells and analyzed priming of CTLs in NOG mice. Half of the mice engrafted with bulk lymphocytes including CD4$^+$ T cells died before analysis probably due to xenoreactive graft versus host disease. All of the mice engrafted with purified CD8$^+$ T cells survived until the analysis, and successful engraftment was observed in 80% of recipient mice. Thus, transfer of purified CD8$^+$ T cells is sufficient and safer than that of bulk lymphocytes. To add antigenic stimulation to the CD8$^+$ T cells in vivo, injection of antigenic peptide-loaded and monocyte-derived autologous dendritic cells (DCs) was simultaneously done and repeated 7 days later. The DC-based vaccinization resulted in efficient priming of HLA class I-restricted and MART1, WT1 or CMV peptides-specific CTLs in the recipient mice. This system may be useful to evaluate the stimulation of antigen-specific human CTLs in vivo.



## 1. Introduction

Studies on anti-cancer immunotherapy have been widely carried out because of its potential merits [1]. One of the major breakthrough in the field was the identification of target antigens expressed in human cancer tissues that could be specifically recognized by cytotoxic T lymphocytes (CTLs) [2]. Many tumor associated antigens (TAAs) and their HLA class I-restricted epitopes have been identified by intensive studies in this decade [3]. It has become apparent that the selection of target antigens is crucial for the efficacy of anti-cancer immunotherapy. In addition, development of means to efficiently prime TAA-specific human T cells in vivo is essential. Dendritic cells (DCs), the most potent antigen presenting cells, are responsible for priming of antigen-specific T cells in the initiation of immune response [4]. In studies using mice, in vivo transfer of antigen-loaded DCs as cellular vaccine has been established to be efficient in priming of antigen-specific CTLs [5]. DC-based methods are regarded as promising strategy of active immunization for clinical anti-cancer immunotherapy [6].

For the analysis of human hematopoiesis and development of immune system in vivo, a number of xenotransplantation models have been tried in that human hematopoietic or immune system was reconstituted in immunocompromised mice [7,8]. Advances in the development of humanized mice have depended on a systematic progression of genetic modifications to establish immunocompromised host mice [9,10]. Non-obese diabetic/SCID (NOD/SCID) mice have been shown to support higher levels of human hematopoietic cell engraftment [11,12]. Several investigators have established the NOD/SCID mice models that were repopulated with human peripheral blood lymphocytes (hu-PBL-NOD/SCID mice). By using these mice, they succeeded in priming in vivo of human immune cells with the viral antigens by administration of the autologous DCs and demonstrated effective antiviral immune response in vivo [13,14]. But the use of humanized NOD/SCID mice remains limited by the residual activity of NK cells and other components of innate immunity, which impedes the engraftment of the human lymphoid compartment.

NOD/Shi-scid IL2rγ$^{null}$ (NOG) mice, which are double homozygous for SCID mutation and interleukin-2 receptor γ chain mutation, are lacking NK cell activity as well as T cells and B cells, and accept human cells more readily than NOD/SCID mice do [15–18]. NOG mice have been used as a good recipient for human cell transplantation [18], and a highly relevant translational model for induction of human immune response in vivo [19,20].

In the present study, we established a NOG mouse-based xenotransplantation model to analyze in vivo priming of human CTLs by human monocyte-derived DCs loaded with TAA-derived peptides.

* Corresponding author. Tel.: +81 96 373 5310; fax: +81 96 373 5314.
*E-mail address:* mxnishim@gpo.kumamoto-u.ac.jp (Y. Nishimura).

0165-2478/$ – see front matter © 2009 Elsevier B.V. All rights reserved.
doi:10.1016/j.imlet.2009.08.001

## 2. Materials and methods

### 2.1. Mice

NOG mice purchased from the Central Institute for Experimental Animals (Kawasaki, Japan) and maintained at the Center for Animal Resources and Development of Kumamoto University were handled in accordance with the animal care policy of Kumamoto University. Mice were 6 weeks old at the time of transfer of human peripheral blood mononuclear cells (PBMCs)-derived cells.

### 2.2. Human blood samples

The plan for experiments using human blood samples was approved by the Institutional Review Board of Kumamoto University. We obtained blood samples from a donor after receiving a written informed consent. Blood samples from a single healthy donor positive for both HLA-A2 (*A*0201*) and HLA-A24 (*A*2402*) were used for all of the experiments in this study. PBMCs were isolated from the whole heparinized blood by means of Ficoll-Conray density gradient centrifugation [21].

### 2.3. Peptides and cytokines

HLA-A2 (*A*0201*)-restricted MART1 peptide p27-35 (AAGIGILTV) was synthesized by F-MOC method, purified by HPLC, and confirmed for molecular weight by using mass spectrometry. HLA-24 (*A*2402*)-restricted modified WT1 peptide p235-243 (CYTWNQMNL), and HLA-A24 (*A*2402*)-restricted cytomegalovirus (CMV) pp65 peptide p341-349 (QYDPVAALF), HLA-A2 (*A*0201*)-restricted HIV Gag peptide p77-85 (SLYNTYATL) and HLA-A24(*A*2402*)-restricted HIV Nef peptide p138-147 (RYPLTFGWCF) were purchased from AnyGen (Korea). Recombinant human GM-CSF, IL-4, and IL-2 were purchased from PeproTech (London, UK).

### 2.4. Generation of dendritic cells from peripheral blood monocytes (Mo-DCs)

Monocytes were isolated from human PBMCs using anti-CD14 monoclonal antibody (mAb)-coated microbeads (Miltenyi Biotec, Tokyo, Japan) and cultured in RPMI-1640 supplemented with 10% heat-inactivated autologous plasma, 100 ng/ml GM-CSF (Peprotech), and 10 ng/ml IL-4 (Peprotech) as described previously [21]. On day 5, OK-432 (Chugai Pharmaceutical, Tokyo, Japan) was added at the concentration of 0.1 KE/ml to induce maturation of Mo-DCs. On day 7, resulting mature Mo-DCs were harvested, incubated with antigenic peptides (10 μM) for 2 h, washed, and used for in vivo transfer.

### 2.5. Transplantation experiments

$CD8^+$ T cells were isolated from PBMCs by positive selection using anti-CD8 microbeads. $CD14^-$ cells were isolated as flow-through cells in the selection with anti-CD14 microbeads, thus including all mononuclear cells other than monocytes. $CD8^+$ T cells ($1 \times 10^7$) or $CD14^-$ cells ($1 \times 10^7$) were mixed with Mo-DCs ($5 \times 10^5$), pre-loaded with antigenic peptide, and intraperitoneally (i.p.) injected into NOG mice. 7 days after the injection, Mo-DCs ($5 \times 10^5$) pulsed with antigenic peptide were i.p. injected again. 14 days after the first injection, mice were sacrificed and spleen cells were harvested. Harvested spleen cells were treated with erythrocyte lysis buffer (0.83% ammonium chloride/20 mM Hepes, pH 7.2) for 1 min and washed with phosphate buffered saline (PBS). Human $CD8^+$ T cells and $CD4^+$ T cells in the spleen cells were detected by flow cytometry. For ex vivo analysis, $CD8^+$ T cells were isolated from harvested spleen cells by positive selection using anti-CD8 microbeads. Production of INF-γ upon co-culture with stimulator cells pre-loaded with antigenic peptides was analyzed by enzyme-linked immunosorbent spot (ELISPOT) assay (BD Biosciences, San Jose, CA) (effector cells: $1 \times 10^5$/well, stimulator cells: $1 \times 10^4$/well, T2 or C1R-A*2402). T2 cell, a TAP-deficient cell harboring HLA-A2 (*A*0201*) gene, was incubated in 26 °C overnight before using for stimulator cells. C1R-A*2402 is a EBV-transformed human B lymphoblastoid cell line expressing very low levels of HLA class I molecules other than HLA-A24 and transfected with the expression vector of HLA-A24 (*A*2402*) gene [22].

### 2.6. ELISA

The sera of the NOG mice were obtained at 2 days and 7 days after the second immunization, and human IFN-γ levels were measured by standard ELISA methods by using human IFN-γ Immunoassay Kit (Invitrogen, Camarillo, CA).

### 2.7. Flow cytometry

Human cells i.p. injected into NOG mice and spleen cells isolated from NOG mice engrafted with $CD8^+$ or $CD14^-$ human lymphocytes were incubated for 1 h at 4 °C with phycoerythrin (PE)-conjugated anti-human CD8a mAb (clone: RPA-T8, BioLegend, San Diego, CA) and fluoresceinisothiocyanate (FITC)-conjugated human CD4 mAb (clone: RPA-T4, BioLegend), or PE-conjugated anti-human CD56 mAb (clone: MEM-188, BioLegend) and FITC-conjugated anti-human TCRαβ mAb (T10B9.1A–31, BD biosciences, San Jose, CA), washed and suspended in PBS, and analyzed on FACScan equipped with CellQuest software (BD).

### 2.8. Preparation of phytohemagglutinin-stimulated blastic cells (PHA blasts)

$CD8^+$ T cells and $CD14^+$ monocytes were serially isolated from PBMCs and residual cell fraction was cultured in AIM-V (Gibco-Invitrogen, Tokyo, Japan) containing 2% heat-inactivated autologous plasma, phytohemagglutinin (PHA, 1 μg/ml) and human recombinant IL-2 (100 units/ml). After 2-days culture, the cells were washed and incubated in the same medium without PHA for further 4 days. Resulting blastic lymphocytes were immediately used as stimulator cells for CTL-culture or stocked frozen for future use.

### 2.9. In vitro amplification of antigen-specific CTLs

To amplify in vivo primed antigen-specific CTL in NOG mice, $CD8^+$ T cells were isolated from the spleen cells by using anti-CD8 microbeads and co-culture with the antigenic peptide loaded and X-ray-irradiated (100 Gy) PHA-blast cells. $2 \times 10^6$ $CD8^+$ T cells and $1 \times 10^6$ PHA-blast cells were cultured in a well of 24-well plate in AIM-V supplemented with 2% human plasma and human recombinant IL-2 (100 units/ml) for 6 days.

### 2.10. Cytotoxicity assay

To prepare target cells, *HLA-A*0201*-expressing *TAP*-deficient human T cell line (T2) was incubated at 26 °C overnight, and labeled with sodium [$^{51}$Cr]-chromate for 1 h at 26 °C and washed. Subsequently, the cells were incubated in 24-well plates ($5 \times 10^5$ cells/well) with or without 10 μM MART1 peptide for 3 h at 26 °C, washed, and seeded into 96-well round-bottomed culture plates ($5 \times 10^3$ cells/well). The cultured $CD8^+$ cells as effector cells were added to the target cells according to the indicated *E*/*T* ratio and incubated for 4 h at 37 °C. At the end of the incubation, supernatants (50 μl/well) were harvested and counted on a gamma counter

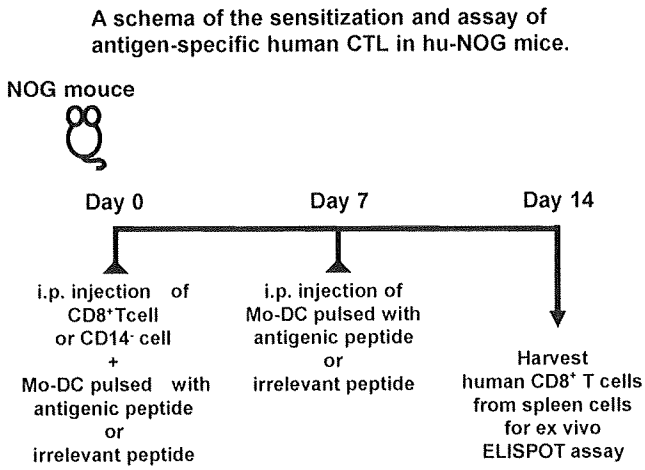


**Fig. 1.** The schema of the sensitization and assay of antigen-specific human CTLs in hu-NOG mice.

(Wallac, GMI, Inc. Ramsey, MN). The percentage of specific lysis was calculated as: $100 \times [(\text{experimental release} - \text{spontaneous release})/(\text{maximal release} - \text{spontaneous release})]$. The spontaneous release and maximal release were determined in the presence of medium alone and PBS-1% Triton X-100, respectively.

### 2.11. Statistical analysis

Two-tailed Student's *t*-test was used to evaluate the statistical significance of differences in the data obtained by the ELISPOT assay. A value of $P < 0.05$ was considered to be significant.

## 3. Results

### 3.1. Engraftment of human peripheral blood T lymphocytes into NOG mice

In the present study, we tried to establish a xenogenic cell transplantation model to analyze stimulation of TAA-specific human CTLs in vivo in NOG mice. We isolated human PBMCs from a healthy donor, sorted certain cell fractions by using microbeads, and i.p. injected the cells into the mice (Fig. 1). At first, we injected whole lymphocytes, containing $CD4^+$ T cells, $CD8^+$ T cells, B cells, NK cells and NKT cells (9–17%) (Fig. 2A and C), along with autologous DCs pre-loaded with antigenic peptides. At 14 days after the injection, $CD8^+$ and $CD4^+$ human T cells were detected in the spleen in 2 out of 4 NOG mice injected (Fig. 2E), indicating successful engraftment of human T cells into these mice. However, the remaining 2 mice out of the 4 mice died before the analysis (Table 1).

Considering that mouse death was due to xenoreactive GVHD probably caused by human $CD4^+$ T cells and NK cells in the injected cells, we purified $CD8^+$ T cells from PBMCs as shown in Fig. 1B and D, and i.p. injected them into NOG mice. In this condition, all of the 20 injected mice survived until the analysis (Table 1). No or very few human $CD8^+$ T cells were detected in the spleen of 4 mice out of the 20 mice. However, in the remaining 16 mice, a substantial number of human $CD8^+$ T cells ($0.3–2.1 \times 10^7$, mean $0.8 \times 10^7$/spleen,

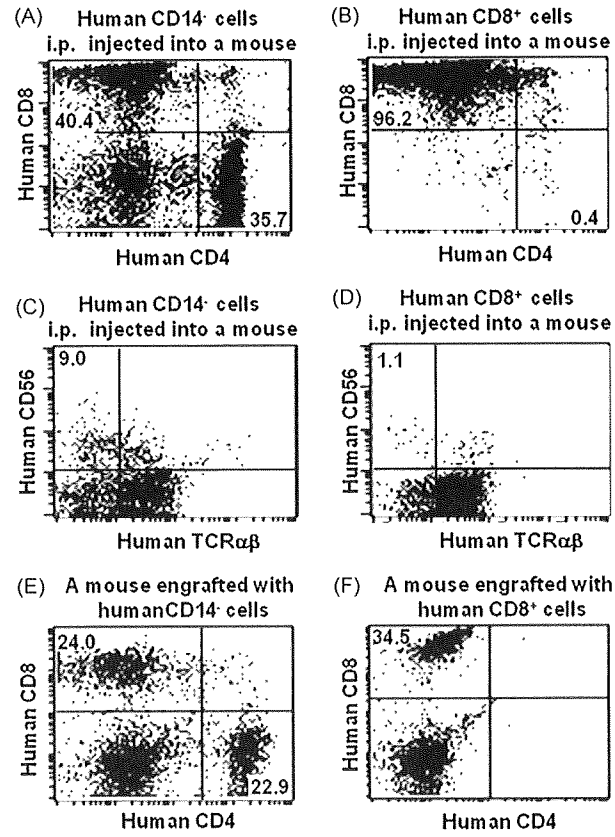


**Fig. 2.** Flow cytometric analysis to detect human T cells in the xenotransplanted NOG mice. Bulk lymphocytes prepared by exclusion of $CD14^+$ cells from PBMCs and including whole T cells, B cells, and NK cells (A) or $CD8^+$ T cells purified from PBMCs (B) were i.p. injected into NOG mice. The flow cytometric analyzes of the expression of human CD56 or TCRαβ on the cells injected into the NOG mice were also shown to estimate the frequency of NK and NKT cells (C, D). On day 14, the mice were sacrificed and human T cells in the spleen cells were analyzed by flow cytometry (E, F). The numbers in the figure indicate the frequency (%) of human cells observed in the indicated quadrant.

11–36% of spleen cells, mean 23%) were detected in the spleen (Fig. 2F), indicating successful engraftment of human $CD8^+$ T cells. Because $CD8^+$ cells injected into NOG mice contained around 1% of human $CD56^+$ $TCR\alpha\beta^-$ NK cells (Fig. 2D), we investigated the frequency of $CD56^+$ human NK cells in the spleen cells of some mice and almost no NK cells were detected in these mice (data not shown). These results suggest that we can analyze priming status of transplanted human $CD8^+$ T cells in the 80% of the NOG mice transplanted with purified human $CD8^+$ T cells.

Based on these results, we concluded that transplantation of purified $CD8^+$ T cells is sufficient and safer than that of bulk lymphocyte preparation, which include $CD4^+$ T cells and NK cells.

### 3.2. Stimulation of human $CD8^+$ T cells specific to tumor antigen or virus antigen in NOG mice

We examined whether antigen-specific human CTLs could be primed in NOG mice in the conditions as described above. MART1

**Table 1**
Summary of the outcome of xenotransplantation of human lymphocytes into NOG mice.

| Cells inoculated | Number of mice | | | |
|---|---|---|---|---|
| | Successful engraftment | Failure of engraftment | Death before day 14 | Total |
| CD 14- cells (whole lymphocytes) | 2 | 0 | 2 | 4 |
| CD8+ T cells | 16 | 4 | 0 | 20 |

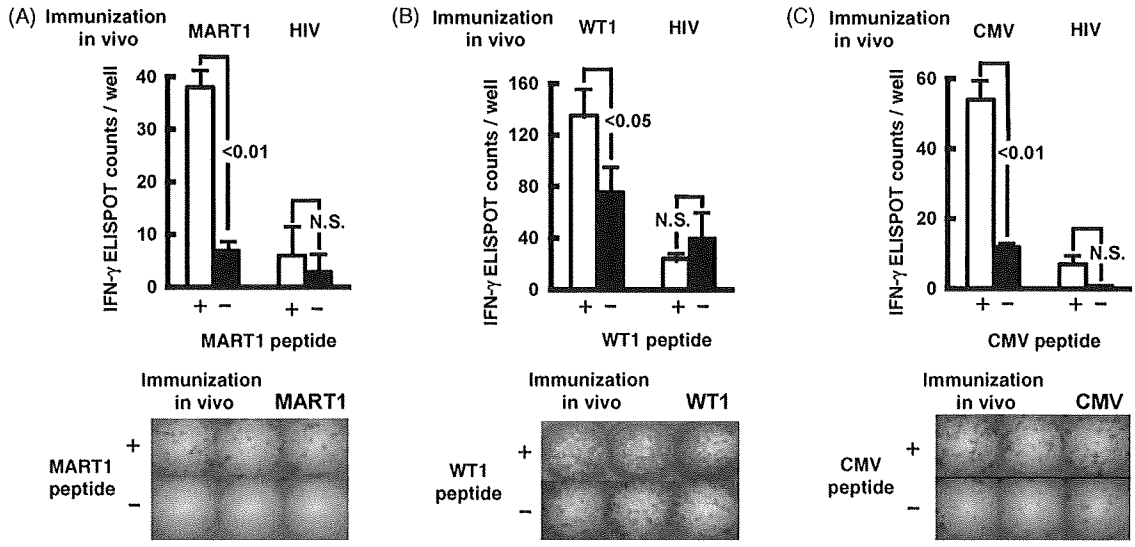


**Fig. 3.** Induction of antigen-specific human CTL in NOG mice engrafted with human CD8⁺ T cells. Human CTLs primed in vivo in NOG mice with HLA-A2 (*A*0201*)-restricted MART1 peptide (A), HLA-A24 (*A*2402*)-restricted WT1 peptide (B), and HLA-A24 (*A*2402*)-restricted CMV peptide (C) were analyzed. The photo images of ELISPOT assay (upper columns) and quantified spot counts (lower columns) in the presence of peptide-pulsed and peptide-unpulsed stimulator cells are shown. CD8⁺ T cells from the same donor were primed with HIV peptide in vivo as negative control. Spot counts are indicated as mean spot counts per well ±SD of the triplicate assays.

and WT1 are typical, well-established human solid tumor- or leukemia-associated antigens. We tried to prime human CTLs specific to HLA-A2 (*A*0201*)-restricted MART1-derived peptide and those specific to HLA-A24 (*A*2402*)-restricted WT1-derived peptide. In addition, we also examined stimulation of HLA-A24 (*A*2402*)-restricted CMV-pp65-peptide-specific CTLs. We injected human CD8⁺ T cells i.p. into NOG mice along with Mo-DCs pulsed with the antigenic peptides (day 0). On day 7, we injected DCs pulsed with the same peptides again. The spleen cells were harvested on day 14, and in vivo priming of the peptide-specific CTLs was analyzed by ELISPOT assays detecting IFN-γ-producing cell upon stimulation with C1R-A*2402 cells or T2 cells pre-loaded with the antigenic peptides.

As shown in Fig. 3A, MART1 peptide-reactive CD8⁺ T cells were detected in the spleen of MART1-immunized mice. On the other hand, CD8⁺ T cells reactive to MART1 peptide were not detected in the spleen of mice immunized with HIV-derived peptide in the same way. Thus, it was demonstrated that MART1 peptide-reactive CD8⁺ T cells were induced by stimulation of human CD8⁺ T cell population by MART1-peptide-loaded Mo-DC in vivo. In addition, CD8⁺ T cells specific to HLA-A24 (*A*2402*)-restricted WT1-derived peptide and those specific to HLA-A24 (*A*2402*)-restricted CMV-derived peptide were also successfully induced (Fig. 3B, C). We observed inductions of peptide-reactive human CD8⁺ CTLs in vivo in 2 out of 4 mice immunized with human Mo-DCs pulsed with the MART1 peptide, 1 out of 2 mice immunized with human Mo-DCs pulsed with the WT1 peptide, and 2 out of 4 mice immunized with human Mo-DCs pulsed with the CMV peptide. One representative data for each antigenic peptide is shown in Fig. 3.

We also measured serum human IFN-γ levels in NOG mice injected with human CD8⁺ cells and Mo-DCs pulsed with the MART1 or WT1 peptides. At 2 days and 7 days after the second i.p. injections of Mo-DCs pulsed with the antigenic peptides, we collected the sera from NOG mice and measured human IFN-γ levels by ELISA. The human IFN-γ was detected in two mice which were injected with human CD8⁺ cells and Mo-DCs pulsed with the MART1 or WT1 peptides. The human IFN-γ levels in these two mice at 2 days after boost immunization were 40 and 80 pg/ml respectively. On the other hand, human IFN-γ levels in two mice injected with human CD8⁺ cells alone were 30 and 40 pg/ml respectively. The human IFN-γ levels were slightly higher in the former group of the NOG mice in comparison to the latter group of the NOG mice. However, the statistical significance of the differences in serum human IFN-γ levels was not observed between these two groups of NOG mice. The serum human IFN-γ levels in these mice at 7 days after the boost immunization were markedly lower than those at 2 days.

### 3.3. *In vitro expansion of MART1-specific human CTLs induced in NOG mice*

We next tried in vitro amplification of in vivo primed antigen-specific CTLs and analyzed the cytotoxic activity of CTLs. We transplanted NOG mice with CD8⁺ T cells and simulated them twice in vivo with HLA-A24 (*A*2402*)-binding MART1-peptide-loaded Mo-DCs, as described above. We purified CD8⁺ T cells from the spleen cells of the mice and co-cultured them with PHA-stimulated blastic cells obtained from the same donor and pre-loaded with the MART1 peptide, as stimulators, for 6 days. As shown in Fig. 4A, a dramatic amplification of MART1-reactive CTLs was observed. The mean numbers of cultured CD8⁺ CTLs were about 6–10 folds higher than those observed before starting in vitro culture. We also analyzed the MART1-specific cytotoxic activity of the cultured cells by Cr-release assay using T2 cells pulsed with the peptide as targets cells. As shown in Fig. 4B, the cells recovered from the amplification culture showed marked killing activity against the MART1-peptide-loaded target cells but not peptide unpulsed cells. We demonstrated in vitro propagation of MART1 reactive CTLs after in vivo priming in 2 out of 2 NOG mice.

## 4. Discussion

In recent years, a number of TAAs have been identified. These antigens are potentially good targets for anti-cancer immunotherapy [23]. To establish truly effective anti-cancer immunotherapy, development of means for potently polarizing the immune system toward these TAAs is essential.

DCs play a crucial role in maintaining immune systems and are particularly efficient in presenting antigenic peptides in the context of MHC to T cells [4]. Thus, DCs generated from peripheral blood monocytes (Mo-DCs) have been used in numbers of clinical trials of cancer therapy. To improve the anti-cancer immunotherapy using

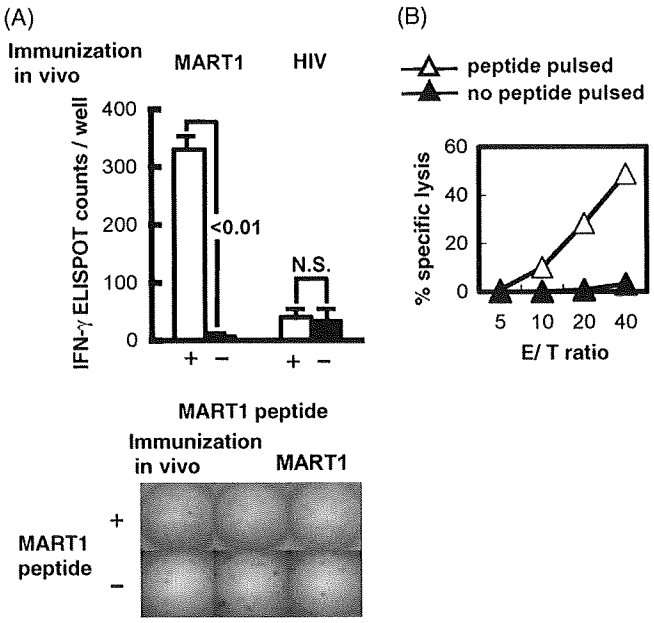


**Fig. 4.** In vitro amplification of MART1-specific human CTLs induced in vivo in NOG mice. $CD8^+$ T cells were primed with HLA-A2 (*A*0201*)-restricted MART1 peptide as done in Fig. 3. 14 days after the T cells injection, spleen cells were recovered from the mice and co-cultured with PHA-stimulated blastic lymphocytes prepared from the same donor and pre-loaded with MART1 peptide. After 6 days, cultured cells were recovered and analyzed on the frequency of IFN-γ-producing cells upon re-stimulation with the MART1 peptide. The photo images of ELISPOT assay and spot counts quantified are shown (A). The cells recovered from the amplification culture showed marked killing activity against the MART1-peptide-loaded target cells but not peptide unpulsed cells by Cr release assay (B).

Mo-DCs, methods for pre-clinical study to evaluate the efficiency of priming of cancer-antigen-specific human CTLs in vivo is need to be established.

Xenotransplantation of human peripheral blood lymphocytes (PBLs) into SCID mice, was first described by Mosier et al. in 1988 [8]. In the later studies, the efficiency of engraftment of human lymphocytes cells was improved by more than 3- to 5-fold higher by using NOD/SCID (hu-PBL-NOD/SCID) mice instead of conventional hu-PBL-SCID mice [24]. There are many studies demonstrating humoral and cellular immune response against viral infections developed in hu-PBL-NOD/SCID mice. Several studies demonstrated the antigen specific immune response against HIV by administration of DCs into hu-PBL-NOD/SCID mice [13,14]. However, due to NK cell activity in NOD/SCID mice, administration of the NK cell-depleting agents was used to avoid human cell-rejection by mouse NK cells in some of these studies.

NOG mice are known to readily accept engrafted human hematopoietic and immune cells. The most attractive characteristic of NOG mice is that human hematopoietic cells develop with high engraftment and have been shown to be able to survive for a long time with the transfer of human umbilical cord blood $CD34^+$ stem cells (hu-HSC NOG mice) [25,26]. After human hematopoietic stem cell transfer to NOG mice, human CD4 single positive and human CD8 single positive cells can be detected in the peripheral blood and spleen. These T cells are considered to be functionally active [17,27]. However there are only a few evidences proving that T cells developed from HSC in hu-HSC NOG mice really recognized human HLA class I-restricted antigenic peptides and show specific response. This may be due to that the T cells developed in the NOG mice are differentiated in the mouse thymus and selected by mouse MHC [28]. Therefore, introduction of *HLA* genes into the mice is necessary to provide a more complete form of human immune system in the mice [18].

In the current study, we used NOG mice as recipients and transplanted mature human T cells instead of HSCs. We i.p. injected human PBLs into NOG mice (hu-PBL NOG mice) as previously described [29]. This model has been used as an in vivo model for viral infection of human T cells, such as HIV or HTLV-1 infection [30,31]. At the beginning of this study, we tried to find out what kind of cell preparation was the best to be transferred into NOG mice. Intending to make an environment in the mouse body that allows production of cytokines and physiological cell-to-cell contact mimicking human immune system, we first tested whole human PBMCs. In this condition, half of mice did not survive until the analysis. The death of mice was considered to be due to GVHD caused by human-to-mouse xenoreactive response of helper T cells and NK cells.

Secondly, we tested transplantation of purified $CD8^+$ T cells. Under this condition, all of the transplanted mice survived for 2 weeks until the analysis. Therefore we decided to transfer purified human $CD8^+$ T cells in the following experiments. However it is well known that in order to fully activate CTLs in vivo the presence of cytokines produced by $CD4^+$ T cells are important [32]. We suggest three possible explanations about the source of cytokines promoting proliferation and activation of human CTLs in our NOG mice. First, the purity of $CD8^+$ T cells injected into NOG mice was about 90–96% and actually our $CD8^+$ T cell fractions were contaminated with 0–3% of $CD4^+$ cells (Fig. 2A). Second, mouse cytokines such as IL-7 cross-reacted to human T cells to induce cell proliferation, because previous study demonstrated that murine IL-7 but not murine IL-15 cross-reacted to human cells [33,34]. Third, it is possible that human $CD8^+$ cells could produce IL-2 by themselves to proliferate in vivo in the NOG mice. According to the results of the present study, the total 14-days schedule with Mo-DC-based vaccination twice with a 7-day-interval and harvest of human CTLs from the mice 7 days after the second immunization is enough to detect in vivo priming of CTLs specific to HLA-restricted antigenic peptides.

In Fig. 3, the ELISPOT counts observed for human $CD8^+$ T cells isolated from the NOG mice in response to peptide-unpulsed stimulator cells are different in each experiment. Moreover, $CD8^+$ T cell response to the CMV peptide was unexpectedly not so much larger than those observed by the stimulation with MART1 or WT1 peptides. We speculate a possible explanation for these phenomena as follows. We frequently observed individual difference in the magnitude of background responses of human CTLs recovered from NOG mice to peptide-unpulsed stimulator cells. The data shown in Fig. 3 were obtained by using PBMCs isolated from three different donors, and as a result, the background CTL responses to the peptide-unpulsed stimulator cells were different in each ELISPOT assay. We also observed the individual differences in responses of CMV-primed and NOG-derived human CTLs to the stimulator cells pulsed with the CMV peptide suggesting that each donor is sensitized in vivo with CMV at a different magnitude. We think these individual differences in $CD8^+$ T cell responses to stimulator cells pulsed with or without the antigenic peptides in a relatively small numbers of experiments caused these observations. To solve this problem, further experiments by using PMMCs isolated from many other different donors are needed in a future.

We are planning to extend our study to establish a model system to analyze the effect to reject primary human tumor cells isolated from cancer patients and transplanted into NOG mice of in vivo primed human CTLs isolated from the same patients. For this purpose, it may be necessary to extend the period of the observation of the NOG mice after the cell transplantation. However, under the experimental conditions so far we established, the half of the mice died between 2 and 3 weeks after the transplantation, even if purified human $CD8^+$ T cells were transferred (data not shown). In this experiment, we transferred Mo-DCs for 3 times with 7-day inter-

vals for immunization and it is possible that excessive activation of the $CD8^+$ T cells may cause the mouse death. To overcome this problem, modification of the experimental protocol may be necessary, for example reducing the number of $CD8^+$ T cells to be transferred or setting the interval between the vaccinations longer than 7 days.

In conclusion, we established in vivo assay system to analyze priming of tumor antigen-specific human CTLs based on xenotransplantation into NOG mice. By using this system, we demonstrated priming of human CTLs specific to MART1, WT1, and CMV peptides. Co-culture in vitro of human $CD8^+$ T cells harvested from mouse spleen with antigenic peptides-loaded autologous PHA-induced blastic lymphocytes was useful to amplify and clearly demonstrate the presence of in vivo primed antigen-specific CTLs. We noticed that transfer of purified human $CD8^+$ T cells was safer than that of bulk lymphocytes, in terms of avoiding early mouse death before analysis. To extend the present study to establish an in vivo model by which we can evaluate the effect of anti-tumor vaccination using TAA peptide-based strategy, further improvement of the experimental procedure is necessary.

## Acknowledgements

This study is supported in part by Grants-in-Aid 16590988, 17390292, 17015035, 18014023, 19591172 and 19059012 from Ministry of Education, Culture, Sport, Science and Technology (MEXT), Japan, the Program of Founding Research Centers for Emerging and Reemerging Infectious Diseases launched as a project commissioned by MEXT, Japan, Research Grant for Intractable Diseases from Ministry of Health, Labour and Welfare, Japan and grants from Japan Science and Technology Agency (JST).

## References

[1] Gattinoni L, Powell DJ, Rosenberg S, Restifo N. Adoptive immunotherapy for cancer: building on success. Nat Rev Immunol 2006;6:383–93.
[2] Boon T, Cerottini J, Van den Eynde B, van der Bruggen P, Van Pel A. Tumor antigens recognized by T lymphocytes. Annu Rev Immunol 1994;12:337–65.
[3] Disis M, Bernhard H, Jaffee E. Use of tumour-responsive T cells as cancer treatment. Lancet 2009;373:673–83.
[4] Guermonprez P, Valladeau J, Zitvogel L, Théry C, Amigorena S. Antigen presentation and T cell stimulation by dendritic cells. Annu Rev Immunol 2002;20:621–67.
[5] Fong L, Engleman E. Dendritic cells in cancer immunotherapy. Annu Rev Immunol 2000;18:245–73.
[6] Berger T, Schultz E. Dendritic cell-based immunotherapy. Curr Top Microbiol Immunol 2003;276:163–97.
[7] McCune J, Namikawa R, Kaneshima H, Shultz L, Lieberman M, Weissman I. The SCID-hu mouse: murine model for the analysis of human hematolymphoid differentiation and function. Science 1988;241:1632–9.
[8] Mosier D, Gulizia R, Baird S, Wilson D. Transfer of a functional human immune system to mice with severe combined immunodeficiency. Nature 1988;335:256–9.
[9] Bosma G, Custer R, Bosma M. A severe combined immunodeficiency mutation in the mouse. Nature 1983;301:527–30.
[10] Shultz L, Schweitzer P, Christianson S, Gott B, Schweitzer I, Tennent B, et al. Multiple defects in innate and adaptive immunologic function in NOD/LtSz-scid mice. J Immunol 1995;154:180–91.
[11] Greiner D, Shultz L, Yates J, Appel M, Perdrizet G, Hesselton R, et al. Improved engraftment of human spleen cells in NOD/LtSz-scid/scid mice as compared with C.B-17-scid/scid mice. Am J Pathol 1995;146:888–902.
[12] Hesselton R, Greiner D, Mordes J, Rajan T, Sullivan J, Shultz L. High levels of human peripheral blood mononuclear cell engraftment and enhanced susceptibility to human immunodeficiency virus type 1 infection in NOD/LtSz-scid/scid mice. J Infect Dis 1995;172:974–82.
[13] Yoshida A, Tanaka R, Murakami T, Takahashi Y, Koyanagi Y, Nakamura M, et al. Induction of protective immune responses against R5 human immunodeficiency virus type 1 (HIV-1) infection in hu-PBL-SCID mice by intrasplenic immunization with HIV-1-pulsed dendritic cells: possible involvement of a novel factor of human CD4(+) T-cell origin. J Virol 2003;77:8719–28.
[14] Gorantla S, Santos K, Meyer V, Dewhurst S, Bowers W, Federoff H, et al. Human dendritic cells transduced with herpes simplex virus amplicons encoding human immunodeficiency virus type 1 (HIV-1) gp120 elicit adaptive immune responses from human cells engrafted into NOD/SCID mice and confer partial protection against HIV-1 challenge. J Virol 2005;79:2124–32.
[15] Ito M, Hiramatsu H, Kobayashi K, Suzue K, Kawahata M, Hioki K, et al. NOD/SCID/gamma(c)(null) mouse: an excellent recipient mouse model for engraftment of human cells. Blood 2002;100:3175–82.
[16] Hiramatsu H, Nishikomori R, Heike T, Ito M, Kobayashi K, Katamura K, et al. Complete reconstitution of human lymphocytes from cord blood CD34+ cells using the NOD/SCID/gammacnull mice model. Blood 2003;102:873–80.
[17] Ishikawa F, Yasukawa M, Lyons B, Yoshida S, Miyamoto T, Yoshimoto G, et al. Development of functional human blood and immune systems in NOD/SCID/IL2 receptor {gamma} chain(null) mice. Blood 2005;106:1565–73.
[18] Ito M, Kobayashi K, Nakahata T. NOD/Shi-scid IL2rgamma(null) (NOG) mice more appropriate for humanized mouse models. Curr Top Microbiol Immunol 2008;324:53–76.
[19] Ito R, Shiina M, Saito Y, Tokuda Y, Kametani Y, Habu S. Antigen-specific antibody production of human B cells in NOG mice reconstituted with the human immune system. Curr Top Microbiol Immunol 2008;324:95–107.
[20] Koyanagi Y, Tanaka Y, Ito M, Yamamoto N. Humanized mice for human retrovirus infection. Curr Top Microbiol Immunol 2008;324:133–48.
[21] Komori H, Nakatsura T, Senju S, Yoshitake Y, Motomura Y, Ikuta Y, et al. Identification of HLA-A2- or HLA-A24-restricted CTL epitopes possibly useful for glypican-3-specific immunotherapy of hepatocellular carcinoma. Clin Cancer Res 2006;12:2689–97.
[22] Karaki S, Kariyone A, Kato N, Kano K, Iwakura Y, Takiguchi M. HLA-B51 transgenic mice as recipients for production of polymorphic HLA-A, B-specific antibodies. Immunogenetics 1993;37:139–42.
[23] Rosenberg S, Yang J, Restifo N. Cancer immunotherapy: moving beyond current vaccines. Nat Med 2004;10:909–15.
[24] Koyanagi Y, Tanaka Y, Kira J, Ito M, Hioki K, Misawa N, et al. Primary human immunodeficiency virus type 1 viremia and central nervous system invasion in a novel hu-PBL-immunodeficient mouse strain. J Virol 1997;71:2417–24.
[25] Yahata T, Ando K, Nakamura Y, Ueyama Y, Shimamura K, Tamaoki N, et al. Functional human T lymphocyte development from cord blood CD34+ cells in nonobese diabetic/Shi-scid, IL-2 receptor gamma null mice. J Immunol 2002;169:204–9.
[26] Watanabe S, Ohta S, Yajima M, Terashima K, Ito M, Mugishima H, et al. Humanized NOD/SCID/IL2Rgamma(null) mice transplanted with hematopoietic stem cells under nonmyeloablative conditions show prolonged life spans and allow detailed analysis of human immunodeficiency virus type 1 pathogenesis. J Virol 2007;81:13259–64.
[27] Shultz L, Lyons B, Burzenski L, Gott B, Chen X, Chaleff S, et al. Human lymphoid and myeloid cell development in NOD/LtSz-scid IL2R gamma null mice engrafted with mobilized human hemopoietic stem cells. J Immunol 2005;174:6477–89.
[28] Saito Y, Kametani Y, Hozumi K, Mochida N, Ando K, Ito M, et al. The in vivo development of human T cells from CD34(+) cells in the murine thymic environment. Int Immunol 2002;14:1113–24.
[29] Miyazato P, Yasunaga J, Taniguchi Y, Koyanagi Y, Mitsuya H, Matsuoka M. De novo human T-cell leukemia virus type 1 infection of human lymphocytes in NOD-SCID, common gamma-chain knockout mice. J Virol 2006;80:10683–91.
[30] Nakata H, Maeda K, Miyakawa T, Shibayama S, Matsuo M, Takaoka Y, et al. Potent anti-R5 human immunodeficiency virus type 1 effects of a CCR5 antagonist, AK602/ONO4128/GW873140, in a novel human peripheral blood mononuclear cell nonobese diabetic-SCID, interleukin-2 receptor gamma-chain-knocked-out AIDS mouse model. J Virol 2005;79:2087–96.
[31] Dewan M, Uchihara J, Terashima K, Honda M, Sata T, Ito M, et al. Efficient intervention of growth and infiltration of primary adult T-cell leukemia cells by an HIV protease inhibitor, ritonavir. Blood 2006;107:716–24.
[32] Kalams S, Walker B. The critical need for CD4 help in maintaining effective cytotoxic T lymphocyte responses. J Exp Med 1998;188:2199–204.
[33] Barata J, Silva A, Abecasis M, Carlesso N, Cumano A, Cardoso A. Molecular and functional evidence for activity of murine IL-7 on human lymphocytes. Exp Hematol 2006;34:1133–42.
[34] Huntington N, Legrand N, Alves N, Jaron B, Weijer K, Plet A, et al. IL-15 trans-presentation promotes human NK cell development and differentiation in vivo. J Exp Med 2009;206:25–34.

# Multiple Antigen-targeted Immunotherapy With α-Galactosylceramide–loaded and Genetically Engineered Dendritic Cells Derived From Embryonic Stem Cells

*Satoshi Fukushima,*† ‡ Shinya Hirata,* Yutaka Motomura,* Daiki Fukuma,* Yusuke Matsunaga,*‡ Yoshiaki Ikuta,* Tokunori Ikeda,*‡ Toshiro Kageshita,† Hironobu Ihn,† Yasuharu Nishimura,* and Satoru Senju*‡*

**Summary:** Numerous tumor-associated antigens (TAA) have been identified and their use in immunotherapy is considered to be promising. For TAA-based immunotherapy to be broadly applied as standard anticancer medicine, methods for active immunization should be improved. In the present study, we demonstrated the efficacy of multiple TAA-targeted dendritic cell (DC) vaccines and also the additive effects of loading α-galactosylceramide to DC using mouse melanoma models. On the basis of previously established methods to generate DC from mouse embryonic stem cells (ES-DC), 4 kinds of genetically modified ES-DC, which expressed the melanoma-associated antigens, glypican-3, secreted protein acidic and rich in cysteine, tyrosinase-related protein-2, or gp100 were generated. Anticancer effects elicited by immunization with the ES-DC were assessed in preventive and also therapeutic settings in the models of peritoneal dissemination and spontaneous metastasis to lymph node and lung. The in vivo transfer of a mixture of 3 kinds of TAA-expressing ES-DC protected the recipient mice from melanoma cells more effectively than the transfer of ES-DC expressing single TAA, thus demonstrating the advantage of multiple as compared with single TAA-targeted immunotherapy. Loading ES-DC with α-galactosylceramide further enhanced the anticancer effects, suggesting that excellent synergic effects of TAA-specific cytotoxic T lymphocytes and natural killer T cells against metastatic melanoma can be achieved by using genetically modified ES-DC. With the aid of advancing technologies related to pluripotent stem cells, induced pluripotent stem cells, and ES cells, clinical application of DC highly potent in eliciting anticancer immunity will be realized in the near future.

**Key Words:** cancer immunotherapy, dendritic cells, embryonic stem cells, tumor-associated antigen, α-GalCer

(*J Immunother* 2009;00:000–000)

A number of preclinical studies have demonstrated the efficacy of cancer vaccines using mouse models. However, cancer vaccine trials in humans have yet to demonstrate a sufficient clinical response,[1,2] and at present tumor-associated antigens (TAA)-specific cancer immunotherapies are not regarded as the standard medical technology, except for several antibody therapies. Therefore, there is discrepancy between the promising results obtained in mouse studies and those of clinical trials. Although the reasons for this discrepancy vary, one is the improper selection of mouse models.[3] Most mouse studies use models where the tumor cells are inoculated subcutaneously or intravenously. These are convenient to observe the efficacy of immunotherapy. However, to evaluate the efficacy in clinical medicine, experimental systems should be used that reflect the clinical situations where immunotherapy is actually needed, such as cancers accompanying with multiple metastases or with peritoneally disseminated lesions. The present study evaluated the capacity of genetically engineered dendritic cells (DC) to inhibit peritoneal dissemination and spontaneous metastasis of mouse melanoma to lymph node and lungs.

Another issue to be considered is whether it is appropriate to design clinical strategies that combine multiple agents to modulate the immune response.[2] Clinically manifested cancers are often associated with multiple mechanisms to evade immune attacks, such as antigen loss, active tolerance induction, deficiency in antigen presentation machineries,[4] etc., which are difficult to be addressed successfully with a single agent. To overcome this defense mechanism and to address the low frequency of cytotoxic T lymphocytes (CTL) that recognize single endogenous TAA, the efficacy of multiple TAA-targeted immunotherapies was examined in the present study. DC were generated expressing endogenous TAA, glypican-3 (GPC3), secreted protein acidic and rich in cysteine (SPARC), tyrosinase-related protein-2 (TRP2), and gp100. The oncofetal protein GPC3, glycosylphosphatidylinositol anchored membrane protein, is specifically overexpressed in human melanoma and hepatocellular carcinoma, and GPC3 can be a candidate target for cancer immunotherapy.[5–7] Clinical trials with GPC3 peptide against hepatocellular carcinoma are now ongoing. SPARC, also called osteonectin, is a matricellular glycoprotein that modulates cellular interactions with the extracellular matrix during tissue remodeling.[8] SPARC or its combination with GPC3 is a useful tumor maker for melanoma.[9,10]

Received for publication August 9, 2008; accepted November 2, 2008.
From the Departments of *Immunogenetics; †Dermatology and Plastic and Reconstructive Surgery, Graduate School of Medical Sciences, Kumamoto University, Kumamoto; and ‡Japan Science and Technology Agency, CREST, Tokyo, Japan.
Financial Disclosure: All of authors have declared there are no financial conflicts of interest related to this work.
Supported in part by Grants-in-Aid 18014023, 19591172, and 19059012 from the Ministry of Education, Science, Technology, Sports, and Culture (MEXT), Japan; the Program of Founding Research Centers for Emerging and Reemerging Infectious Diseases launched as a project commissioned by MEXT, Japan; Research Grant for Intractable Diseases from Ministry of Health and Welfare, Japan and Uehara Memorial Foundation; and Takeda Science Foundation.
Reprints: Satoru Senju, Department of Immunogenetics, Graduate School of Medical Sciences, Kumamoto University, 1-1-1 Honjo, Kumamoto 860-8556, Japan (e-mail: senjusat@gpo.kumamoto-u.ac.jp).